Numerical analysis of a new formulation for the Oseen equations in terms of vorticity and Bernoulli pressure

Verónica Anaya,[*]   David Mora,[†]   Amiya K. Pani,[‡]   Ricardo Ruiz-Baier[§]

July 29, 2020

Abstract

A variational formulation is introduced for the Oseen equations written in terms of vorticity and Bernoulli pressure. The velocity is fully decoupled using the momentum balance equation, and it is later recovered by a post-process. A finite element method is also proposed, consisting in equal-order Nédélec finite elements and piecewise continuous polynomials for the vorticity and the Bernoulli pressure, respectively. The *a priori* error analysis is carried out in the L^2-norm for vorticity, pressure, and velocity; under a smallness assumption either on the convecting velocity, or on the mesh parameter. Furthermore, an *a posteriori* error estimator is designed and its robustness and efficiency are studied using weighted norms. Finally, a set of numerical examples in 2D and 3D is given, where the error indicator serves to guide adaptive mesh refinement. These tests illustrate the behaviour of the new formulation in typical flow conditions, and they also confirm the theoretical findings.

Key words: Oseen equations; vorticity-based formulation; finite element methods; *a priori* error bounds; *a posteriori* error estimation; numerical examples.

Mathematics subject classifications (2000): 65N30, 65N12, 76D07, 65N15

1   Introduction

In this paper, we propose a reformulation of the Oseen equations using only vorticity and Bernoulli pressure. A similar splitting of the unknowns has been recently proposed in [9] for the Brinkman equations. We extend those results for the Oseen problem and propose a residual-based *a posteriori* error estimator whose properties are studied using a weighted energy norm, as well as the L^2-norm.

There is an abundant body of literature dealing with numerical methods for incompressible flow problems using the vorticity as a dedicated unknown. These include spectral elements [6,10], stabilised and least-squares schemes [5,15], and mixed finite elements [8,22–24,30], to name a few. Works specifically devoted to the analysis of numerical schemes for the Oseen equations in terms of vorticity include the non-conforming exponentially accurate least-squares spectral method for Oseen equations proposed in [27], the least-squares method proposed in [32] for Oseen and Navier-Stokes equations, the family of vorticity-based first-order Oseen-type systems studied in [18], the enhanced accuracy formulation in terms of velocity-vorticity-helicity

---

[*]GIMNAP, Departamento de Matemática, Universidad del Bío-Bío, Concepción, Chile; and Centro de Investigación en Ingeniería Matemática (CI²MA), Universidad de Concepción, Concepción, Chile. E-mail: `vanaya@ubiobio.cl`.

[†]GIMNAP, Departamento de Matemática, Universidad del Bío-Bío, Concepción, Chile; and Centro de Investigación en Ingeniería Matemática (CI²MA), Universidad de Concepción, Concepción, Chile. E-mail: `dmora@ubiobio.cl`.

[‡]Department of Mathematics, Indian Institute of Technology Bombay, Powai, Mumbai 400076, India. E-mail: `akp@math.iitb.ac.in`

[§]School of Mathematical Sciences, Monash University, 9 Rainforest Walk, Clayton VIC 3800, Australia. E-mail: `ricardo.ruizbaier@monash.edu`.

investigated in [12], and the recent mixed and DG discretisations for Oseen's problem in velocity-vorticity-pressure form, proposed in [7].

The method advocated in this article focuses on Nédélec elements of order $k \geq 1$ for the vorticity and piecewise continuous polynomials of degree k, for the Bernoulli pressure. An abridged version of the analysis for this formulation has been recently advanced in [3]. In contrast, here we provide details on the *a priori* error estimates rigorously derived for the finite element discretisations in the L^2-norm under enough regularity and under smallness assumption on the mesh parameter. Furthermore, we prove error estimates for two post-processes for the velocity field in the L^2-norm. The first one is similar to the one used in [9] for Brinkman equations, which exploits the momentum equation and direct differentiation of the discrete vorticity and Bernoulli pressure. For the second post-process we solve an additional elliptic problem emanating from the constitutive equation defining vorticity, and it uses the continuity equation and the discrete vorticity appears on the right-hand side. This problem is discretised with, e.g., piecewise linear and continuous polynomials.

On the other hand, we address the construction of residual based *a posteriori* error estimators which are reliable and efficient. Adaptive mesh refinement strategies based on *a posteriori* error indicators have a significant role in computing numerical solutions to partial differential equations, and this is of high importance in the particular context of incompressible flow problems. Robust and efficient error estimators permit to restore the optimal convergence of finite element methods, specifically when complex geometries or singular coefficients are present (which could otherwise lead to non-convergence or to the generation of spurious solutions) [33], and they can provide substantial enhancement to the accuracy of the approximations [1]. *A posteriori* error analyses for vorticity-based equations are already available from the literature (see, e.g., [4, 5, 8, 16]), but considering formulations substantially different to the one we put forward here. Our analysis complements these works by establishing upper and lower bounds in different norms, and using an estimator that is scaled according to the expected regularity of the solutions (which in turn also depends on the regularity of the domain). Reliability of the *a posteriori* error estimator is proved in the L^2-norm, and local efficiency of the error indicator is shown by using a standard technique based on bubble functions.

We further remark that the present method has the advantage of direct computation of vorticity, and it is relatively competitive in terms of computational cost (for instance when compared with the classical MINI-element, or Taylor-Hood schemes). The type of vorticity-based formulations we use here can be of additional physical relevance in scenarios where boundary effects are critical, for example as in those discussed in [21, 28]. Moreover, the corresponding analysis is fairly simple, only requiring classical tools for elliptic problems.

We have structured the contents of the paper in the following manner. We present the model problem as well as the two-field weak formulation and its solvability analysis in Section 2. The finite element discretisation is constructed in Section 3, where we also derive the stability, convergence bounds and we present two post-processes for the velocity field. Section 4 is devoted to the analysis of reliability and efficiency of a weighted residual-based *a posteriori* error indicator, and we close in Section 5 with a set of numerical tests that illustrate the properties of the proposed numerical scheme in a variety of scenarios, including validation of the adaptive refinement procedure guided by the error estimator.

2   The continuous formulation of the Oseen problem

This section deals with some preliminaries, variational formulation for the Oseen problem given in terms of vorticity and Bernoulli pressure and its well-posedness.

2.1   Preliminaries

Let $\Omega \subset \mathbb{R}^3$ be a bounded and connected Lipschitz domain with its boundary $\Gamma = \partial\Omega$ and further, let $\boldsymbol{n}$ be the outward unit vector normal to Γ. The starting point of our investigation is the following form of the

equations, that use velocity, vorticity, and Bernoulli pressure (see, e.g., [7, 29])

$$\sigma \boldsymbol{u} - \nu \Delta \boldsymbol{u} + \mathbf{curl}\,\boldsymbol{u} \times \boldsymbol{\beta} + \nabla p = \boldsymbol{f} \qquad \text{in } \Omega,$$
$$\text{div}\,\boldsymbol{u} = 0 \qquad \text{in } \Omega, \tag{2.1}$$

where $\nu > 0$ is the kinematic viscosity, and a linearisation and backward Euler time stepping explain the terms $\sigma > 0$ as the inverse of the time step, and $\boldsymbol{\beta}$ as an adequate approximation of velocity (representing for example the velocity at a previous time step). The Bernoulli pressure relates to the true fluid pressure P as follows $p := P + \frac{1}{2}\boldsymbol{u} \cdot \boldsymbol{u} - \lambda$, where λ is the mean value of $\frac{1}{2}\boldsymbol{u} \cdot \boldsymbol{u}$.

The structure of (2.1) suggests to introduce the rescaled vorticity vector $\boldsymbol{\omega} := \sqrt{\nu}\,\mathbf{curl}\,\boldsymbol{u}$ as a new unknown. Thus, the Oseen problem can be formulated as: Find $\boldsymbol{u}, \boldsymbol{\omega}, p$ such that

$$\sigma \boldsymbol{u} + \sqrt{\nu}\,\mathbf{curl}\,\boldsymbol{\omega} + \nu^{-1/2}\boldsymbol{\omega} \times \boldsymbol{\beta} + \nabla p = \boldsymbol{f} \qquad \text{in } \Omega, \tag{2.2}$$
$$\boldsymbol{\omega} - \sqrt{\nu}\,\mathbf{curl}\,\boldsymbol{u} = \mathbf{0} \qquad \text{in } \Omega, \tag{2.3}$$
$$\text{div}\,\boldsymbol{u} = 0 \qquad \text{in } \Omega, \tag{2.4}$$
$$\boldsymbol{u} = \boldsymbol{g} \qquad \text{on } \Gamma. \tag{2.5}$$

The vector of external forces $\boldsymbol{f}$ absorbs the contributions related to previous time steps and to the fixed states in the linearisation procedure that leads from Navier-Stokes to Oseen equations. Along with to the Dirichlet boundary condition for the velocity on Γ, the additional condition $(p, 1)_{\Omega, 0} = 0$ is required to have uniqueness of the Bernoulli pressure. We will also assume that the data are regular enough: $\boldsymbol{f} \in \mathrm{L}^2(\Omega)^3$ and $\boldsymbol{\beta} \in \mathrm{L}^\infty(\Omega)^3$. However, we do not restrict the behaviour of $\text{div}\,\boldsymbol{\beta}$. For different assumptions on $\boldsymbol{\beta}$ we refer to, e.g., [11, 19, 20, 32].

For the sake of conciseness of the presentation, the analysis in the sequel is carried out for homogeneous boundary conditions on velocity, i.e. $\boldsymbol{g} = \mathbf{0}$ on Γ. Non homogeneous boundary data, as well as mixed boundary conditions, will be considered in the numerical examples in Section 5, below.

2.2 Variational formulation

For any $s \geq 0$, the symbol $\|\cdot\|_{s,\Omega}$ denotes the norm of the Hilbert Sobolev spaces $\mathrm{H}^s(\Omega)$ or $\mathrm{H}^s(\Omega)^3$, with the usual convention $\mathrm{H}^0(\Omega) := \mathrm{L}^2(\Omega)$. For $s \geq 0$, we recall the definition of the space

$$\mathrm{H}^s(\mathbf{curl}; \Omega) := \left\{ \boldsymbol{\theta} \in \mathrm{H}^s(\Omega)^3 : \ \mathbf{curl}\,\boldsymbol{\theta} \in \mathrm{H}^s(\Omega)^3 \right\},$$

endowed with the norm $\|\boldsymbol{\theta}\|_{\mathrm{H}^s(\mathbf{curl};\Omega)} = \left(\|\boldsymbol{\theta}\|_{s,\Omega}^2 + \|\mathbf{curl}\,\boldsymbol{\theta}\|_{s,\Omega}^2 \right)^{1/2}$, and will denote $\mathrm{H}(\mathbf{curl}; \Omega) = \mathrm{H}^0(\mathbf{curl}; \Omega)$. Finally, c and C, with subscripts, tildes, or hats, will represent a generic constant independent of the mesh parameter h.

We denote the function spaces

$$\mathbf{Z} := \mathrm{H}(\mathbf{curl}; \Omega), \qquad \text{and} \qquad \mathrm{Q} := \mathrm{H}^1(\Omega) \cap \mathrm{L}_0^2(\Omega),$$

which are endowed, respectively, with the following norms

$$\|\boldsymbol{\theta}\|_{\mathbf{Z}} := \left(\|\boldsymbol{\theta}\|_{0,\Omega}^2 + \nu \|\mathbf{curl}\,\boldsymbol{\theta}\|_{0,\Omega}^2 \right)^{1/2} \qquad \text{and} \qquad \|q\|_{\mathrm{Q}} := (\|q\|_{0,\Omega}^2 + \|\nabla q\|_{0,\Omega}^2)^{1/2}.$$

Here, $\mathrm{L}_0^2(\Omega)$ represents the set of $\mathrm{L}^2(\Omega)$ functions with mean value zero.

In addition, for sake of the subsequent analysis, it is convenient to introduce the following space

$$\mathbb{V} := \{(\boldsymbol{\theta}, q) \in \mathrm{L}^2(\Omega)^3 \times \mathrm{L}_0^2(\Omega) : \ \sqrt{\nu}\,\mathbf{curl}\,\boldsymbol{\theta} + \nabla q \in \mathrm{L}^2(\Omega)^3\}.$$

Lemma 2.1 *The space $\mathbb{V}$ endowed with the norm defined by*

$$\|(\boldsymbol{\theta}, q)\|_{\mathbb{V}} := \left(\sigma \|\boldsymbol{\theta}\|_{0,\Omega}^2 + \|\sqrt{\nu}\,\mathbf{curl}\,\boldsymbol{\theta} + \nabla q\|_{0,\Omega}^2 + \|q\|_{0,\Omega}^2 \right)^{1/2} \tag{2.6}$$

is a Hilbert space.

Proof. Note that (2.6) is in fact a norm as $\|(\boldsymbol{\theta}, q)\|_{\mathbb{V}} = 0$ implies $(\boldsymbol{\theta}, q) = (\mathbf{0}, 0)$ a.e. Now, it is easy to check that the norm satisfies the parallelogram identity and hence, it induces an inner product by the polarisation identity. Therefore, $\mathbb{V}$ equipped with this inner product is an inner product space. To complete the proof, it remains to show that this space is complete. To this end, let $\{(\boldsymbol{\theta}_n, q_n)\}_{n\in\mathbb{N}}$ be an arbitrary Cauchy sequence in $\mathbb{V}$. From the completeness of $\mathrm{L}^2(\Omega)^3$ and $\mathrm{L}_0^2(\Omega)$, it follows that $(\boldsymbol{\theta}_n, q_n) \to (\hat{\boldsymbol{\theta}}, \hat{q}) \in \mathrm{L}^2(\Omega)^3 \times \mathrm{L}_0^2(\Omega)$ and $\sqrt{\nu}\,\mathbf{curl}\,\boldsymbol{\theta}_n + \nabla q_n \to \boldsymbol{\varphi} \in \mathrm{L}^2(\Omega)^3$. We now observe that $\sqrt{\nu}\,\mathbf{curl}\,\hat{\boldsymbol{\theta}} + \nabla\hat{q} \in \mathcal{D}(\Omega)'$, and for $\boldsymbol{\xi} \in \mathcal{D}(\Omega)$

$$
\begin{aligned}
\langle \sqrt{\nu}\,\mathbf{curl}\,\hat{\boldsymbol{\theta}} + \nabla\hat{q}, \boldsymbol{\xi}\rangle &= \sqrt{\nu}\langle\mathbf{curl}\,\hat{\boldsymbol{\theta}}, \boldsymbol{\xi}\rangle + \langle\nabla\hat{q}, \boldsymbol{\xi}\rangle = \sqrt{\nu}\langle\hat{\boldsymbol{\theta}}, \mathbf{curl}\,\boldsymbol{\xi}\rangle - \langle\hat{q}, \mathrm{div}\,\boldsymbol{\xi}\rangle \\
&= \lim_{n\to\infty} \left[\sqrt{\nu}\langle\hat{\boldsymbol{\theta}}_n, \mathbf{curl}\,\boldsymbol{\xi}\rangle - \langle\hat{q}_n, \mathrm{div}\,\boldsymbol{\xi}\rangle \right] \\
&= \lim_{n\to\infty} \left[\sqrt{\nu}\langle\mathbf{curl}\,\hat{\boldsymbol{\theta}}_n, \boldsymbol{\xi}\rangle + \langle\nabla\hat{q}_n, \boldsymbol{\xi}\rangle \right] \\
&= \langle\boldsymbol{\varphi}, \boldsymbol{\xi}\rangle.
\end{aligned}
$$

Here we have employed integration by parts twice and the continuity of the involved operators in passing to the limit. Therefore, $\sqrt{\nu}\,\mathbf{curl}\,\hat{\boldsymbol{\theta}} + \nabla\hat{q} = \boldsymbol{\varphi} \in \mathrm{L}^2(\Omega)^3$ and this completes the rest of the proof. $\qquad\square$

In order to derive a variational formulation of the problem, we test (2.3) against a sufficiently smooth function $\sigma\boldsymbol{\theta}$. Then, integrating by parts (using the classical curl-based Gauss theorems from, e.g., [25]) and using the velocity boundary condition, we arrive at

$$\sigma\int_\Omega \boldsymbol{\omega}\cdot\boldsymbol{\theta} - \sigma\sqrt{\nu}\int_\Omega \boldsymbol{u}\cdot\mathbf{curl}\,\boldsymbol{\theta} = 0. \tag{2.7}$$

Next, from the momentum equation (2.2), we readily obtain the relation

$$\sigma\boldsymbol{u} = \boldsymbol{f} - \sqrt{\nu}\,\mathbf{curl}\,\boldsymbol{\omega} - \nu^{-1/2}\boldsymbol{\omega}\times\boldsymbol{\beta} - \nabla p \quad \text{in} \quad \Omega, \tag{2.8}$$

and after replacing (2.8) in (2.7), we find that

$$\sigma\int_\Omega \boldsymbol{\omega}\cdot\boldsymbol{\theta} + \nu\int_\Omega \mathbf{curl}\,\boldsymbol{\omega}\cdot\mathbf{curl}\,\boldsymbol{\theta} + \sqrt{\nu}\int_\Omega \nabla p\cdot\mathbf{curl}\,\boldsymbol{\theta} + \int_\Omega (\boldsymbol{\omega}\times\boldsymbol{\beta})\cdot\mathbf{curl}\,\boldsymbol{\theta} = \sqrt{\nu}\int_\Omega \boldsymbol{f}\cdot\mathbf{curl}\,\boldsymbol{\theta}.$$

Next for a given sufficiently smooth function q, we can test (2.2) against ∇q. Then, we integrate by parts and use again the velocity boundary condition, as well as (2.4) to arrive at

$$\sigma\int_\Omega \boldsymbol{u}\cdot\nabla q = 0,$$

which leads to the variational form

$$\sqrt{\nu}\int_\Omega \mathbf{curl}\,\boldsymbol{\omega}\cdot\nabla q + \nu^{-1/2}\int_\Omega (\boldsymbol{\omega}\times\boldsymbol{\beta})\cdot\nabla q + \int_\Omega \nabla p\cdot\nabla q = \int_\Omega \boldsymbol{f}\cdot\nabla q.$$

Summarising, problem (2.2)-(2.5) is written in its weak form as: Find $(\boldsymbol{\omega}, p) \in \mathbb{V}$ such that

$$\mathcal{A}((\boldsymbol{\omega}, p), (\boldsymbol{\theta}, q)) = \mathcal{F}(\boldsymbol{\theta}, q) \quad \forall(\boldsymbol{\theta}, q) \in \mathbb{V}, \tag{2.9}$$

where the multilinear form $\mathcal{A} : \mathbb{V}\times\mathbb{V} \to \mathbb{R}$ and linear functional $\mathcal{F} : \mathbb{V} \to \mathbb{R}$ are specified as

$$\mathcal{A}((\boldsymbol{\omega}, p), (\boldsymbol{\theta}, q)) := \sigma\int_\Omega \boldsymbol{\omega}\cdot\boldsymbol{\theta} + \int_\Omega (\sqrt{\nu}\,\mathbf{curl}\,\boldsymbol{\omega} + \nabla p)\cdot(\sqrt{\nu}\,\mathbf{curl}\,\boldsymbol{\theta} + \nabla q) \tag{2.10}$$

$$+ \nu^{-1/2} \int_\Omega (\boldsymbol{\omega} \times \boldsymbol{\beta}) \cdot (\sqrt{\nu}\,\mathbf{curl}\,\boldsymbol{\theta} + \nabla q),$$

$$\mathcal{F}(\boldsymbol{\theta}, q) := \int_\Omega \boldsymbol{f} \cdot (\sqrt{\nu}\,\mathbf{curl}\,\boldsymbol{\theta} + \nabla q). \tag{2.11}$$

While our whole development will focus on this vorticity-pressure formulation, we stress that from (2.8) we can immediately have an expression for velocity

$$\boldsymbol{u} = \sigma^{-1} \left(\boldsymbol{f} - \nu^{-1/2} \boldsymbol{\omega} \times \boldsymbol{\beta} - (\sqrt{\nu}\,\mathbf{curl}\,\boldsymbol{\omega} + \nabla p) \right) \quad \text{in} \quad \Omega. \tag{2.12}$$

Remark 2.1 *The reason for scaling the vorticity with $\sqrt{\nu}$ is now apparent from the structure of the variational form in (2.10). On the other hand, if we write instead $\bar{\boldsymbol{\omega}} := \mathbf{curl}\,\boldsymbol{u}$, then (2.9) could be written as: Find $(\bar{\boldsymbol{\omega}}, p) \in \mathbb{V}$ such that*

$$\frac{\sigma}{\nu} \int_\Omega \bar{\boldsymbol{\omega}} \cdot \boldsymbol{\theta} + \int_\Omega (\mathbf{curl}\,\bar{\boldsymbol{\omega}} + \nabla p) \cdot (\mathbf{curl}\,\boldsymbol{\theta} + \nabla q) + \nu^{-1} \int_\Omega (\bar{\boldsymbol{\omega}} \times \boldsymbol{\beta}) \cdot (\mathbf{curl}\,\boldsymbol{\theta} + \nabla q)$$

$$= \int_\Omega \boldsymbol{f} \cdot (\mathbf{curl}\,\boldsymbol{\theta} + \nabla q) \quad \forall (\boldsymbol{\theta}, q) \in \mathbb{V},$$

and the analysis of this problem follows the same structure as that of (2.9).

Let us first provide an auxiliary result to be used in the derivation of *a priori* error estimates.

Lemma 2.2 *The multilinear form $\mathcal{A}$ satisfies the following bounds for all $(\boldsymbol{\theta}, q) \in \mathbb{V}$,*

$$\mathcal{A}((\boldsymbol{\theta}, q), (\boldsymbol{\theta}, q)) \geq \sigma \left(1 - \frac{2\|\boldsymbol{\beta}\|_{\infty, \Omega}^2}{\nu \sigma} \right) \|\boldsymbol{\theta}\|_{0, \Omega}^2 + \frac{1}{2} \|\sqrt{\nu}\,\mathbf{curl}\,\boldsymbol{\theta} + \nabla q\|_{0, \Omega}^2, \tag{2.13}$$

$$\mathcal{A}((\boldsymbol{\omega}, p), (\boldsymbol{\theta}, q)) \leq \|(\boldsymbol{\omega}, p)\|_{\mathbb{V}} \|(\boldsymbol{\theta}, q)\|_{\mathbb{V}}. \tag{2.14}$$

Proof. From the definition of $\mathcal{A}(\cdot, \cdot)$, we readily obtain the relation

$$\sigma\|\boldsymbol{\theta}\|_{0, \Omega}^2 + \|\sqrt{\nu}\,\mathbf{curl}\,\boldsymbol{\theta} + \nabla q\|_{0, \Omega}^2 + \nu^{-1/2} \int_\Omega (\boldsymbol{\theta} \times \boldsymbol{\beta}) \cdot (\sqrt{\nu}\,\mathbf{curl}\,\boldsymbol{\theta} + \nabla q) = \mathcal{A}((\boldsymbol{\theta}, q), (\boldsymbol{\theta}, q)).$$

Subsequently, an appeal to the Cauchy-Schwarz inequality leads to

$$\sigma \left(1 - \frac{2\|\boldsymbol{\beta}\|_{\infty, \Omega}^2}{\nu \sigma} \right) \|\boldsymbol{\theta}\|_{0, \Omega}^2 + \frac{1}{2} \|\sqrt{\nu}\,\mathbf{curl}\,\boldsymbol{\theta} + \nabla q\|_{0, \Omega}^2 \leq \mathcal{A}((\boldsymbol{\theta}, q), (\boldsymbol{\theta}, q)). \tag{2.15}$$

Thus, (2.13) follows from (2.15), and relation (2.14) follows directly form the Cauchy-Schwarz inequality. This completes the proof. $\qquad \square$

As a consequence of Lemma 2.2, we can readily derive the following result, stating the stability of problem (2.9).

Lemma 2.3 *Assume that*

$$2\|\boldsymbol{\beta}\|_{\infty, \Omega}^2 < \nu \sigma, \tag{2.16}$$

holds true. Then, there exists $C > 0$ such that

$$\|(\boldsymbol{\omega}, p)\|_{\mathbb{V}} \leq C \|\boldsymbol{f}\|_{0, \Omega}.$$

Proof. Choose $(\boldsymbol{\theta}, q) = (\boldsymbol{\omega}, p)$ in (2.9). From (2.13) with (2.16), and the bound

$$|\mathcal{F}(\boldsymbol{\omega}, p)| \leq \|\boldsymbol{f}\|_{0,\Omega} \|\sqrt{\nu}\, \mathbf{curl}\, \boldsymbol{\omega} + \nabla p\|_{0,\Omega} \leq \|\boldsymbol{f}\|_{0,\Omega} \|(\boldsymbol{\omega}, p)\|_{\mathbb{V}},$$

we obtain

$$\left(\|\boldsymbol{\omega}\|_{0,\Omega}^2 + \|\sqrt{\nu}\, \mathbf{curl}\, \boldsymbol{\omega} + \nabla p\|_{0,\Omega}^2 \right) \leq C\, \|\boldsymbol{f}\|_{0,\Omega} \|(\boldsymbol{\omega}, p)\|_{\mathbb{V}}.$$

Then, we note that

$$\|p\|_{0,\Omega} \leq C_s\, \|\nabla p\|_{-1,\Omega},$$

and invoking the definition of the H^{-1}-norm, it is observed that

$$
\begin{aligned}
\|\nabla p\|_{-1,\Omega} &\leq \sup_{\{q \in \mathrm{H}_0^1(\Omega): \|\nabla q\|_{0,\Omega}=1\}} (\nabla p, \nabla q)_{0,\Omega} \\
&= \sup_{\{q \in \mathrm{H}_0^1(\Omega): \|\nabla q\|_{0,\Omega}=1\}} \left((\sqrt{\nu}\, \mathbf{curl}\, \boldsymbol{\omega} + \nabla p, \nabla q)_{0,\Omega} - (\sqrt{\nu}\, \mathbf{curl}\, \boldsymbol{\omega}, \nabla q)_{0,\Omega} \right).
\end{aligned}
$$

Using integration by parts for the second term in this last relation, and using that $q \in \mathrm{H}_0^1(\Omega)$ as well as $\nabla \cdot \mathbf{curl}\, \boldsymbol{\omega} = 0$, $(\sqrt{\nu}\, \mathbf{curl}\, \boldsymbol{\omega}, \nabla q) = 0$, we end up with

$$
\begin{aligned}
\|p\|_{0,\Omega} \leq C_s \|\nabla p\|_{-1,\Omega} &\leq C_s\, \|\sqrt{\nu}\, \mathbf{curl}\, \boldsymbol{\omega} + \nabla p\|_{0,\Omega} \\
&\leq C_s\, \|(\boldsymbol{\omega}, p)\|_{\mathbb{V}}.
\end{aligned}
\tag{2.17}
$$

Altogether, it completes the rest of the proof. $\qquad \square$

Theorem 2.1 *Under the assumption* (2.16)*, there exists a unique weak solution* $(\boldsymbol{\omega}, p) \in \mathbb{V}$ *to the problem* (2.9)*, which depends continuously on* $\boldsymbol{f}$*.*

Proof. The continuous dependence of the solution $(\boldsymbol{\omega}, p) \in \mathbb{V}$ on the given data $\boldsymbol{f}$ is a consequence of the stability Lemma 2.3. Likewise, a straightforward application of that result implies the uniqueness of solution.

On the other hand, for the existence we note that the multilinear form $\mathcal{A}(\cdot, \cdot)$ is both coercive and bounded in $\mathbb{V}$ with respect to $\|(\cdot, \cdot)\|_{\mathbb{V}}$ because of Lemmas 2.2 and 2.3. Therefore, an appeal to the Lax-Milgram Lemma completes the rest of the proof. $\qquad \square$

Remark 2.2 *Even if* $\boldsymbol{\beta}$ *violates* (2.16) *we can still address the well-posedness of problem* (2.9)*. Since problem* (2.1) *with the boundary conditions* $\boldsymbol{u} = \boldsymbol{0}$ *on* Γ *is equivalent to* (2.9) *under the assumption of sufficient regularity, then the unique solvability of* (2.1) *implies that of* (2.9)*. Now, denoting by* $\mathbf{P}$ *the Leray projection operator that maps* $\boldsymbol{L}^2$ *onto a divergence-free space, we can see that the following problem*

$$\mathcal{L}(\boldsymbol{u}) := \mathbf{P}(-\nu \Delta \boldsymbol{u} + \mathbf{curl}\, \boldsymbol{u} \times \boldsymbol{\beta} + \sigma \boldsymbol{u} + \nabla p) = \mathbf{P}\boldsymbol{f},$$

defines a Fredholm alternative (see for instance, [17]). Note also that, as long as zero is not in the spectrum of $\mathcal{L}$*, the operator* $\mathcal{L}$ *is invertible. With the null space of* $\mathcal{L}$ *being a trivial space, the operator* $\mathcal{L}$ *is indeed an isomorphism onto the dual space* $\mathbf{Z}'$ *of* $\mathbf{Z}$*. Finally,* p *is recovered in a standard way.*

In any case, for the rest of the paper we will simply assume that

(A) The problem (2.9) has a unique weak solution $(\boldsymbol{\omega}, p) \in \mathbb{V}$.

3 Finite element discretisation and error estimates

This section focuses on finite element approximations and their *a priori* error estimates.

3.1 Galerkin scheme and solvability

Let $\{\mathcal{T}_h(\Omega)\}_{h>0}$ be a shape-regular family of partitions of the polyhedral region $\bar{\Omega}$, by tetrahedrons T of diameter h_T, with mesh size $h := \max\{h_T : T \in \mathcal{T}_h(\Omega)\}$. In what follows, given an integer $k \geq 1$ and a subset S of $\mathbb{R}^3$, $\mathcal{P}_k(S)$ will denote the space of polynomial functions defined locally in S and being of total degree $\leq k$.

Now, for any $T \in \mathcal{T}_h(\Omega)$ we recall the definition of the local Nédélec space

$$\mathbb{N}_k(T) := \mathcal{P}_{k-1}(T)^3 \oplus R_k(T),$$

where $R_k(T) := \{\boldsymbol{p} \in \bar{\mathcal{P}}_k(T)^3 : \boldsymbol{p}(\boldsymbol{x}) \cdot \boldsymbol{x} = 0\}$, and where $\bar{\mathcal{P}}_k$ is the subset of homogeneous polynomials of degree k. With this we define the discrete spaces for vorticity and Bernoulli pressure:

$$
\begin{aligned}
\mathbf{Z}_h &:= \{\boldsymbol{\theta}_h \in \mathbf{Z} : \boldsymbol{\theta}_h|_T \in \mathbb{N}_k(T) \quad \forall T \in \mathcal{T}_h(\Omega)\}, \\
\mathrm{Q}_h &:= \{q_h \in \mathrm{Q} : q_h|_T \in \mathcal{P}_k(T) \quad \forall T \in \mathcal{T}_h(\Omega)\}, \\
\mathbb{V}_h &:= \mathbf{Z}_h \times \mathrm{Q}_h,
\end{aligned}
\tag{3.1}
$$

and remark that functions in $\mathbf{Z}_h$ have continuous tangential components across the faces of $\mathcal{T}_h(\Omega)$.

Let us recall that for $s > 1/2$, the Nédélec global interpolation operator $\mathcal{N}_h : \mathrm{H}^s(\mathbf{curl};\Omega) \to \mathbf{Z}_h$ (cf. [2]), satisfies the following approximation property: For all $\boldsymbol{\theta} \in \mathrm{H}^s(\mathbf{curl};\Omega)$ with $s \in (1/2, k]$, there exists $C_{\mathrm{apx}} > 0$ independent of h, such that

$$\|\boldsymbol{\theta} - \mathcal{N}_h\boldsymbol{\theta}\|_{\mathbf{Z}} \leq C_{\mathrm{apx}}\, h^s \|\boldsymbol{\theta}\|_{\mathrm{H}^s(\mathbf{curl};\Omega)}.\tag{3.2}$$

On the other hand, for all $s > 1/2$, the usual Lagrange interpolant $\Pi_h : \mathrm{H}^{1+s}(\Omega) \cap \mathrm{Q} \to \mathrm{Q}_h$ features a similar property. Namely: For all $q \in \mathrm{H}^{1+s}(\Omega)$, $s \in (1/2, k]$ there exists $C_{\mathrm{apx}} > 0$, independent of h, such that

$$\|q - \Pi_h q\|_{\mathrm{Q}} \leq C_{\mathrm{apx}}\, h^s \|q\|_{\mathrm{H}^{1+s}(\Omega)}.\tag{3.3}$$

The Galerkin approximation of (2.9) reads: *Find $(\boldsymbol{\omega}_h, p_h) \in \mathbb{V}_h$ such that*

$$\mathcal{A}((\boldsymbol{\omega}_h, p_h), (\boldsymbol{\theta}_h, q_h)) = \mathcal{F}(\boldsymbol{\theta}_h, q_h) \quad \forall(\boldsymbol{\theta}_h, q_h) \in \mathbb{V}_h,\tag{3.4}$$

where the multilinear form $\mathcal{A} : \mathbb{V}_h \times \mathbb{V}_h \to \mathbb{R}$ and the linear functional $\mathcal{F} : \mathbb{V}_h \to \mathbb{R}$ are specified as in (2.10) and (2.11), respectively.

Next, let us prove that the discrete formulation (3.4) is well-posed.

Before that, we address the stability of the discrete problem.

Lemma 3.1 *Under the assumption (A), and $h > 0$ small enough, there exists $C > 0$, independent of h, such that*

$$\|(\boldsymbol{\omega}_h, p_h)\|_{\mathbb{V}} \leq C\, \|\boldsymbol{f}\|_{0,\Omega}.$$

Proof. Choosing $(\boldsymbol{\theta}_h, q_h) = (\boldsymbol{\omega}_h, p_h)$ in (3.4), a use of the Cauchy-Schwarz inequality with the estimate

$$\nu^{-1/2}\int_\Omega (\boldsymbol{\omega}_h \times \boldsymbol{\beta}) \cdot (\sqrt{\nu}\,\mathbf{curl}\,\boldsymbol{\omega}_h + \nabla p_h) \leq 2\,\nu^{-1/2}\,\|\boldsymbol{\beta}\|_{\infty,\Omega}\|\boldsymbol{\omega}_h\|_{0,\Omega}\|\sqrt{\nu}\,\mathbf{curl}\,\boldsymbol{\omega}_h + \nabla p_h\|_{0,\Omega},$$

yields

$$\sigma\|\boldsymbol{\omega}_h\|_{0,\Omega}^2 + \|\sqrt{\nu}\,\mathbf{curl}\,\boldsymbol{\omega}_h + \nabla p_h\|_{0,\Omega}^2 \leq \left(\|\boldsymbol{f}\|_{0,\Omega} + 2\,\nu^{-1/2}\|\boldsymbol{\beta}\|_{\infty,\Omega}\|\boldsymbol{\omega}_h\|_{0,\Omega}\right)\|\sqrt{\nu}\,\mathbf{curl}\,\boldsymbol{\omega}_h + \nabla p_h\|_{0,\Omega}.\tag{3.5}$$

By (2.17), it follows that

$$\|p_h\|_{0,\Omega} \leq C_s\, \|\sqrt{\nu}\,\mathbf{curl}\,\boldsymbol{\omega}_h + \nabla p_h\|_{0,\Omega}.$$

And eventually we arrive at

$$\|(\boldsymbol{\omega}_h, p_h)\|_{\mathbb{V}} \leq C \left(\|\boldsymbol{f}\|_{0,\Omega} + \sigma^{-1/2}\, \nu^{-1/2}\sigma^{1/2}\|\boldsymbol{\beta}\|_{\infty,\Omega}\|\boldsymbol{\omega}_h\|_{0,\Omega} \right). \tag{3.6}$$

In order to complete the proof, we require an estimate for $\sigma^{1/2}\|\boldsymbol{\omega}_h\|_{0,\Omega}$. For this we apply the Aubin-Nitsche duality argument to the following adjoint problem: Find $(\widetilde{\boldsymbol{\omega}}, \widetilde{p}) \in \mathbf{Z} \times \mathrm{Q}$ such that

$$\mathcal{A}((\boldsymbol{\theta}, q), (\widetilde{\boldsymbol{\omega}}, \widetilde{p})) = \sigma(\boldsymbol{\omega}_h, \boldsymbol{\theta})_{0,\Omega} + (p_h, q)_{0,\Omega} \qquad \forall (\boldsymbol{\theta}, q) \in \mathbf{Z} \times \mathrm{Q},$$

and whose solution (after assuming the natural additional regularity $\widetilde{\boldsymbol{\omega}} \in \mathrm{H}^{\delta}(\mathbf{curl}; \Omega)$ and $\widetilde{p} \in \mathrm{H}^{1+\delta}(\Omega)$, for some $\delta \in (1/2, 1]$) satisfies

$$\|\widetilde{\boldsymbol{\omega}}\|_{\mathrm{H}^{\delta}(\mathbf{curl},\Omega)} + \|\widetilde{p}\|_{\mathrm{H}^{1+\delta}(\Omega)} \leq C_{\mathrm{reg}}(\sigma^{1/2}\|\boldsymbol{\omega}_h\|_{0,\Omega} + \|p_h\|_{0,\Omega}),$$

for $C_{\mathrm{reg}} > 0$ a uniform regularity constant. Then, we set $(\boldsymbol{\theta}, q) = (\boldsymbol{\omega}_h, p_h)$ and find out that for all $(\boldsymbol{\theta}_h, q_h) \in \mathbf{Z}_h \times \mathrm{Q}_h$, the following relation holds:

$$\begin{aligned}
\sigma \, \|\boldsymbol{\omega}_h\|_{0,\Omega}^2 + \|p_h\|_{0,\Omega}^2 &= \mathcal{A}((\boldsymbol{\omega}_h, p_h), (\widetilde{\boldsymbol{\omega}}, \widetilde{p})) = \mathcal{A}((\boldsymbol{\omega}_h, p_h), (\widetilde{\boldsymbol{\omega}} - \boldsymbol{\theta}_h, \widetilde{p} - q_h)) - \mathcal{F}(\widetilde{\boldsymbol{\omega}} - \boldsymbol{\theta}_h, \widetilde{p} - q_h) + \mathcal{F}(\widetilde{\boldsymbol{\omega}}, \widetilde{p}) \\
&\leq \sigma\|\boldsymbol{\omega}_h\|_{0,\Omega}\|\widetilde{\boldsymbol{\omega}} - \boldsymbol{\theta}_h\|_{0,\Omega} + \left(\|\sqrt{\nu}\,\mathbf{curl}\,\widetilde{\boldsymbol{\omega}} + \nabla\widetilde{p}\|_{0,\Omega} + \|\sqrt{\nu}\,\mathbf{curl}(\widetilde{\boldsymbol{\omega}} - \boldsymbol{\theta}_h) + \nabla(\widetilde{p} - q_h)\|_{0,\Omega} \right) \|\boldsymbol{f}\|_{0,\Omega} \\
&\quad + \left(\|\sqrt{\nu}\,\mathbf{curl}\,\boldsymbol{\omega}_h + \nabla p_h\|_{0,\Omega} + \nu^{-1/2}\|\boldsymbol{\beta}\|_{\infty,\Omega}\|\boldsymbol{\omega}_h\|_{0,\Omega} \right) \|\sqrt{\nu}\,\mathbf{curl}(\widetilde{\boldsymbol{\omega}} - \boldsymbol{\theta}_h) + \nabla(\widetilde{p} - q_h)\|_{0,\Omega} \\
&\leq C_{\mathrm{reg}}\, C_{\mathrm{apx}} \left(\sigma\|\boldsymbol{\omega}_h\|_{0,\Omega}^2 + \|p_h\|_{0,\Omega}^2 \right)^{1/2} \left(h^{\delta} \left(1 + \sigma^{1/2} + \sigma^{-1/2}\,\nu^{-1/2}\|\boldsymbol{\beta}\|_{\infty,\Omega}\right) \|(\boldsymbol{\omega}_h, p_h)\|_{\mathbb{V}} + \|\boldsymbol{f}\|_{0,\Omega} \right).
\end{aligned}$$

In this way, we obtain

$$\left(\sigma\|\boldsymbol{\omega}_h\|_{0,\Omega}^2 + \|p_h\|_{0,\Omega}^2 \right)^{1/2} \leq C_{\mathrm{reg}}\, C_{\mathrm{apx}} \left(h^{\delta} \left(1 + \sigma^{1/2} + \sigma^{-1/2}\,\nu^{-1/2}\|\boldsymbol{\beta}\|_{\infty,\Omega}\right) \|(\boldsymbol{\omega}_h, p_h)\|_{\mathbb{V}} + \|\boldsymbol{f}\|_{0,\Omega} \right), \tag{3.7}$$

and on substitution of (3.7) into (3.6), we readily see that

$$\left(1 - C_s\, C_{\mathrm{reg}}\, C_{\mathrm{apx}}\, \sigma^{-1/2}\, \nu^{-1/2} \left(1 + \sigma^{1/2} + \sigma^{-1/2}\, \nu^{-1/2}\|\boldsymbol{\beta}\|_{\infty,\Omega}\right) h^{\delta} \right) \|(\boldsymbol{\omega}_h, p_h)\|_{\mathbb{V}} \leq C\, \|\boldsymbol{f}\|_{0,\Omega}.$$

Therefore, there is a positive h_0 such that for $0 < h \leq h_0$, the following holds:

$$\left(1 - C_s\, C_{\mathrm{reg}}\, C_{\mathrm{apx}}\, \sigma^{-1/2}\, \nu^{-1/2} \left(1 + \sigma^{1/2} + \sigma^{-1/2}\, \nu^{-1/2}\|\boldsymbol{\beta}\|_{\infty,\Omega}\right) h^{\delta} \right) \geq \gamma_0 > 0,$$

for some positive γ_0, independent of h. This completes the rest of the proof. $\qquad\square$

Theorem 3.1 *For $h > 0$ small enough, the discrete problem* (3.4) *has a unique solution* $(\boldsymbol{\omega}_h, p_h) \in \mathbb{V}_h$.

Proof. Since the assembled discrete problem (3.4) is a square linear system, it is enough to establish uniqueness of solution. Considering $\boldsymbol{f} = \mathbf{0}$ and using $(\boldsymbol{\theta}_h, q_h) := (\boldsymbol{\omega}_h, p_h)$ as a test function in (3.4), the discrete stability result in Lemma 3.1 (which is valid assuming (2.16)) immediately implies that $\boldsymbol{\omega}_h = \mathbf{0}$ and $p_h = 0$, thus concluding the proof. $\qquad\square$

Remark 3.1 *When the condition* (2.16) *is satisfied, we modify the stability proof of Lemma 3.1 as follows: From* (3.5), *using the Young inequality on the right-hand side*

$$\sigma\left(1 - \frac{2\|\boldsymbol{\beta}\|_{\infty,\Omega}^2}{\sigma\nu}\right)\|\boldsymbol{\omega}_h\|_{0,\Omega}^2 + \frac{1}{2}\|\sqrt{\nu}\,\mathbf{curl}\,\boldsymbol{\omega}_h + \nabla p_h\|_{0,\Omega}^2 \leq \|\boldsymbol{f}\|_{0,\Omega}^2.$$

In addition, applying Young's inequality once again, and appealing to (2.17), *we obtain the desired stability result.*

Note that in this case, we do not need a smallness condition on the mesh parameter h.

3.2 *A priori* error estimates

In this subsection, using a classical duality argument we bound the error measured in the L^2-norm by the error in the norm $\|(\cdot,\cdot)\|_{\mathbb{V}}$. Then, we establish an energy error estimate that eventually yields an optimal bound in L^2.

Let $(\boldsymbol{\omega}, p) \in \mathbb{V}$ and $(\boldsymbol{\omega}_h, p_h) \in \mathbb{V}_h$ be the unique solutions to the continuous and discrete problems (cf. (2.9) and (3.4)), respectively. Then, we obtain

$$\mathcal{A}((\boldsymbol{\omega} - \boldsymbol{\omega}_h, p - p_h), (\boldsymbol{\theta}_h, q_h)) = 0 \quad \forall (\boldsymbol{\theta}_h, q_h) \in \mathbb{V}_h. \tag{3.8}$$

Lemma 3.2 (An L^2-estimate) *There exists $C > 0$, independent of h, such that for h small enough, and $\delta \in (1/2, 1]$*

$$\|\boldsymbol{\omega} - \boldsymbol{\omega}_h\|_{0,\Omega} + \|p - p_h\|_{0,\Omega} \le C\, h^\delta\, \|(\boldsymbol{\omega} - \boldsymbol{\omega}_h, p - p_h)\|_{\mathbb{V}}.$$

Proof. We appeal again to the Aubin-Nitsche duality argument. For this, let us consider the adjoint continuous problem: Find $(\widetilde{\boldsymbol{\omega}}, \widetilde{p}) \in \mathbb{V}$ such that

$$\mathcal{A}((\boldsymbol{\theta}, q), (\widetilde{\boldsymbol{\omega}}, \widetilde{p})) = (\sigma(\boldsymbol{\omega} - \boldsymbol{\omega}_h), \boldsymbol{\theta})_{0,\Omega} + (p - p_h, q)_{0,\Omega} \quad \forall (\boldsymbol{\theta}, q) \in \mathbb{V}. \tag{3.9}$$

In addition, let us suppose that (3.9) is well-posed and that $\widetilde{\boldsymbol{\omega}} \in \mathrm{H}^\delta(\mathbf{curl}; \Omega)$ and $\widetilde{p} \in \mathrm{H}^{1+\delta}(\Omega)$, and there exists a constant $C_{\mathrm{reg}} > 0$, such that

$$\|\widetilde{\boldsymbol{\omega}}\|_{\mathrm{H}^\delta(\mathbf{curl},\Omega)} + \|\widetilde{p}\|_{\mathrm{H}^{1+\delta}(\Omega)} \le C_{\mathrm{reg}}(\sigma^{1/2}\|\boldsymbol{\omega} - \boldsymbol{\omega}_h\|_{0,\Omega} + \|p - p_h\|_{0,\Omega}). \tag{3.10}$$

Next, we proceed to test the adjoint problem (3.9) against $(\boldsymbol{\theta}, q) := (\boldsymbol{\omega} - \boldsymbol{\omega}_h, p - p_h)$ and to use the error equation (3.8) with $(\boldsymbol{\theta}_h, q_h) = (\mathcal{N}_h\widetilde{\boldsymbol{\omega}}, \Pi_h\widetilde{p}) \in \mathbb{V}_h$ to obtain that

$$
\begin{aligned}
\sigma\, \|\boldsymbol{\omega} - \boldsymbol{\omega}_h\|_{0,\Omega}^2 + \|p - p_h\|_{0,\Omega}^2 &= \mathcal{A}((\boldsymbol{\omega} - \boldsymbol{\omega}_h, p - p_h), (\widetilde{\boldsymbol{\omega}}, \widetilde{p})) \\
&= \mathcal{A}((\boldsymbol{\omega} - \boldsymbol{\omega}_h, p - p_h), (\widetilde{\boldsymbol{\omega}} - \boldsymbol{\theta}_h, \widetilde{p} - q_h)) \\
&\le \left(1 + \sigma^{1/2} + \sigma^{-1/2}\, \nu^{-1/2}\|\boldsymbol{\beta}\|_{\infty,\Omega}\right) \|(\boldsymbol{\omega} - \boldsymbol{\omega}_h, p - p_h)\|_{\mathbb{V}}\|(\widetilde{\boldsymbol{\omega}} - \boldsymbol{\theta}_h, \widetilde{p} - q_h)\|_{\mathbb{V}} \\
&\le C_{\mathrm{reg}}C_{\mathrm{apx}}h^\delta\left(1 + \sigma^{1/2} + (\sigma\nu)^{-1/2}\|\boldsymbol{\beta}\|_{\infty,\Omega}\right)\|(\boldsymbol{\omega} - \boldsymbol{\omega}_h, p - p_h)\|_{\mathbb{V}}\left(\|\boldsymbol{\omega} - \boldsymbol{\omega}_h\|_{0,\Omega}^2 + \|p - p_h\|_{0,\Omega}^2\right)^{1/2}.
\end{aligned}
$$

Here, we have used (3.2) and (3.3) with $s = \delta$ and this completes the rest of the proof. $\qquad\square$

An error estimate in the energy norm can also be derived in the following manner.

Theorem 3.2 *Assume that problem* (2.9) *has a unique solution* $(\boldsymbol{\omega}, p)$ *satisfying the additional regularity* $\boldsymbol{\omega} \in \mathrm{H}^s(\mathbf{curl}; \Omega)$ *and* $p \in \mathrm{H}^{1+s}(\Omega)$, *for some* $s \in (1/2, k]$. *Then, there exists* $C > 0$, *independent of* h, *such that the following error estimates hold for* h *small enough:*

$$\|(\boldsymbol{\omega} - \boldsymbol{\omega}_h, p - p_h)\|_{\mathbb{V}} \le C\, h^s\left(\|\boldsymbol{\omega}\|_{\mathrm{H}^s(\mathbf{curl};\Omega)} + \|p\|_{\mathrm{H}^{1+s}(\Omega)}\right),$$

$$\|\boldsymbol{\omega} - \boldsymbol{\omega}_h\|_{0,\Omega} + \|p - p_h\|_{0,\Omega} \le C\, h^{s+\delta}\left(\|\boldsymbol{\omega}\|_{\mathrm{H}^s(\mathbf{curl};\Omega)} + \|p\|_{\mathrm{H}^{1+s}(\Omega)}\right),$$

where $(\boldsymbol{\omega}_h, p_h) \in \mathbb{V}_h$ *is the unique solution to* (3.4) *with* $s = \delta$, *if* $s \in (1/2, 1)$ *and* $\delta = 1$, *if* $s \in [1, k]$.

Proof. Now rewrite (3.8), then use boundedness, (3.2) and (3.3) to arrive at

$$
\begin{aligned}
\mathcal{A}((\boldsymbol{\omega} - \boldsymbol{\omega}_h, p - p_h), (\boldsymbol{\omega} - \boldsymbol{\omega}_h, p - p_h)) &= \mathcal{A}((\boldsymbol{\omega} - \boldsymbol{\omega}_h, p - p_h), (\boldsymbol{\omega} - \mathcal{N}_h\boldsymbol{\omega}, p - \Pi_h p)) \\
&\le C\, \|(\boldsymbol{\omega} - \boldsymbol{\omega}_h, p - p_h)\|_{\mathbb{V}}\, \|(\boldsymbol{\omega} - \mathcal{N}_h\boldsymbol{\omega}, p - \Pi_h p)\|_{\mathbb{V}} \\
&\le C\, h^s\|(\boldsymbol{\omega} - \boldsymbol{\omega}_h, p - p_h)\|_{\mathbb{V}}\left(\|\boldsymbol{\omega}\|_{\mathrm{H}^s(\mathbf{curl};\Omega)} + \|p\|_{\mathrm{H}^{1+s}(\Omega)}\right).
\end{aligned}
\tag{3.11}
$$

Next, for the term on the left-hand side of (3.11), apply (2.13) to obtain

$$\mathcal{A}((\boldsymbol{\omega} - \boldsymbol{\omega}_h, p - p_h), (\boldsymbol{\omega} - \boldsymbol{\omega}_h, p - p_h))$$
$$\geq 1/2 \left(\|(\boldsymbol{\omega} - \boldsymbol{\omega}_h, p - p_h)\|_{\mathbb{V}}^2 - (1 + \sigma^{-1}\, \nu^{-1}\, \|\boldsymbol{\beta}\|_\infty)\, (\sigma\|\boldsymbol{\omega} - \boldsymbol{\omega}_h\|_{0,\Omega}^2 + \|p - p_h\|_{0,\Omega}^2) \right).$$

Then, a use of Lemma 3.2 yields

$$\mathcal{A}((\boldsymbol{\omega} - \boldsymbol{\omega}_h, p - p_h), (\boldsymbol{\omega} - \boldsymbol{\omega}_h, p - p_h))$$
$$\geq 1/2 \left(1 - C(1 + \sigma^{-1}\, \nu^{-1}\, \|\boldsymbol{\beta}\|_\infty)\, h^{2\delta} \right) \|(\boldsymbol{\omega} - \boldsymbol{\omega}_h, p - p_h)\|_{\mathbb{V}}^2.$$

Choosing h small, the term within brackets, $(1 - C(1 + \sigma^{-1}\, \nu^{-1}\, \|\boldsymbol{\beta}\|_\infty)\, h^{2\delta})$, can be made positive; therefore, concluding the proof. $\qquad\square$

As a consequence of Theorem 3.2, with $e_{\boldsymbol{\omega}} := \boldsymbol{\omega} - \boldsymbol{\omega}_h$ and $e_p := p - p_h$, we obtain the following inf-sup condition: There exists $\gamma_0 > 0$, independent of h, such that,

$$\sup_{(\boldsymbol{\theta}, q) \in \mathbb{V}} \frac{\mathcal{A}((e_{\boldsymbol{\omega}}, e_p), (\boldsymbol{\theta}, q))}{\|(\boldsymbol{\theta}, q)\|_{\mathbb{V}}} \geq \gamma_0\, \|(e_{\boldsymbol{\omega}}, e_p)\|_{\mathbb{V}}. \tag{3.12}$$

3.3 Convergence of the post-processed velocity

Let $(\boldsymbol{\omega}_h, p_h) \in \mathbb{V}_h$ be the unique solution of the discrete problem (3.4). Then following (2.12), we can recover the discrete velocity as the following element-wise discontinuous function for each $T \in \mathcal{T}_h(\Omega)$:

$$\boldsymbol{u}_h|_T := \sigma^{-1} \left(\mathcal{P}_h \boldsymbol{f} - \nu^{-1/2} \boldsymbol{\omega}_h \times \boldsymbol{\beta} - (\sqrt{\nu}\, \mathbf{curl}\, \boldsymbol{\omega}_h + \nabla p_h) \right)|_T, \tag{3.13}$$

where $\mathcal{P}_h : \mathrm{L}^2(\Omega)^3 \to \mathbf{U}_h$ is the L^2-orthogonal projector, with

$$\mathbf{U}_h := \{\boldsymbol{v}_h \in \mathrm{L}^2(\Omega)^3 : \boldsymbol{v}_h|_T \in \mathcal{P}_{k-1}(T)^3 \quad \forall T \in \mathcal{T}_h(\Omega)\}. \tag{3.14}$$

Consequently, we can state an error estimate for the post-processed velocity.

Theorem 3.3 *Let* $(\boldsymbol{\omega}, p) \in \mathbb{V}$ *be the unique solution of* (2.9), *and* $(\boldsymbol{\omega}_h, p_h) \in \mathbb{V}_h$ *be the unique solution of* (3.4). *Assume that* $\boldsymbol{\omega} \in \mathrm{H}^s(\mathbf{curl}; \Omega)$, $p \in \mathrm{H}^{1+s}(\Omega)$ *and* $\boldsymbol{f} \in \mathrm{H}^s(\Omega)^3$, *for some* $s \in (1/2, k]$. *Then, there exists a positive constant* C, *independent of* h, *such that*

$$\|\boldsymbol{u} - \boldsymbol{u}_h\|_{0,\Omega} \leq C h^s \left(\|\boldsymbol{f}\|_{\mathrm{H}^s(\Omega)} + \|\boldsymbol{\omega}\|_{\mathrm{H}^s(\mathbf{curl}; \Omega)} + \|p\|_{\mathrm{H}^{1+s}(\Omega)} \right).$$

Proof. From (2.12), (3.13), and triangle inequality, it follows that

$$\|\boldsymbol{u} - \boldsymbol{u}_h\|_{0,\Omega}$$
$$\leq \frac{1}{\sigma} \left(\|\boldsymbol{f} - \mathcal{P}_h \boldsymbol{f}\|_{0,\Omega} + \|\sqrt{\nu}\, \mathbf{curl}(\boldsymbol{\omega}_h - \boldsymbol{\omega}) - \nabla(p - p_h)\|_{0,\Omega} + \frac{1}{\sqrt{\nu}} \|(\boldsymbol{\omega} - \boldsymbol{\omega}_h) \times \boldsymbol{\beta}\|_{0,\Omega} \right).$$

Then, the result follows from standard estimates satisfied by $\mathcal{P}_h$, as well as from Theorem 3.2. $\qquad\square$

An issue with the post-process (3.13) is that it requires numerical differentiation (taking the curl of $\boldsymbol{\omega}_h$ and the gradient of p_h). A possible way to getting around this problem is to set

$$\widetilde{\mathbf{U}}_h := \{\boldsymbol{v}_h \in \mathrm{H}_0^1(\Omega)^3 : \boldsymbol{v}_h|_T \in \mathcal{P}_k(T)^3 \quad \forall T \in \mathcal{T}_h(\Omega)\},$$

and recover the discrete velocity in this space, using the discrete versions of (2.3), (2.4), and (2.5).

This results in finding $\tilde{\boldsymbol{u}}_h \in \widetilde{\mathbf{U}}_h$ such that

$$\nu \int_\Omega \mathbf{curl}\, \tilde{\boldsymbol{u}}_h \cdot \mathbf{curl}\, \boldsymbol{v}_h + \nu \int_\Omega \operatorname{div} \tilde{\boldsymbol{u}}_h \, \operatorname{div} \boldsymbol{v}_h = \sqrt{\nu} \int_\Omega \boldsymbol{\omega}_h \cdot \mathbf{curl}\, \boldsymbol{v}_h \qquad \forall \boldsymbol{v}_h \in \widetilde{\mathbf{U}}_h. \tag{3.15}$$

The discrete velocity produced by (3.15) gives not only

$$\|\sqrt{\nu}\, \mathbf{curl}(\boldsymbol{u} - \tilde{\boldsymbol{u}}_h)\|_{0,\Omega} + \|\sqrt{\nu}\, \operatorname{div}(\boldsymbol{u} - \tilde{\boldsymbol{u}}_h)\|_{0,\Omega} = \mathcal{O}(h^s),$$

but also, thanks to the identity relating vector Laplacians with curl and divergence $-\Delta \Phi = \mathbf{curl}\,\mathbf{curl}\,\Phi - \nabla(\operatorname{div}\Phi)$, one can show, using duality arguments, that

$$\|\boldsymbol{u} - \tilde{\boldsymbol{u}}_h\|_{0,\Omega} = \mathcal{O}(h^{s+\delta}),$$

where s and δ are given as in Theorem 3.2.

4   *A posteriori* error analysis for the 2D problem

In this section, we propose a residual-based *a posteriori* error estimator. For sake of clarity, we restrict our analysis to the two-dimensional case (the extension to 3D can be carried out in a similar fashion). Therefore, the functional space $\mathbf{Z}$ considered in the *a priori* error analysis now becomes $\mathbf{Z} := \mathrm{H}^1(\Omega)$, and

$$\mathbf{Z}_h := \{\theta_h \in \mathbf{Z} : \theta_h|_T \in \mathcal{P}_k(T) \quad \forall T \in \mathcal{T}_h(\Omega)\}. \tag{4.1}$$

We note that in the 2D case, the duality arguments presented in Section 3, hold for any $\delta \in (0,1]$. In particular, this fact will be considered in the definition of the local *a posteriori* error indicator. Moreover, to keep the notation clear, in this section we will denote by $\mathcal{N}_h$ the usual Lagrange interpolant in $\mathbf{Z}_h$.

For each $T \in \mathcal{T}_h$ we let $\mathcal{E}(T)$ be the set of edges of T, and we denote by $\mathcal{E}_h$ the set of all edges in $\mathcal{T}_h$, that is

$$\mathcal{E}_h = \mathcal{E}_h(\Omega) \cup \mathcal{E}_h(\Gamma),$$

where $\mathcal{E}_h(\Omega) := \{e \in \mathcal{E}_h : e \subset \Omega\}$, and $\mathcal{E}_h(\Gamma) := \{e \in \mathcal{E}_h : e \subset \Gamma\}$. In what follows, h_e stands for the diameter of a given edge $e \in \mathcal{E}_h$, $\boldsymbol{t}_e = (-n_2, n_1)$, where $\boldsymbol{n}_e = (n_1, n_2)$ is a fix unit normal vector of e. Now, let $q \in \mathrm{L}^2(\Omega)$ such that $q|_T \in C(T)$ for each $T \in \mathcal{T}_h$, then, given $e \in \mathcal{E}_h(\Omega)$, we denote by $[q]$ the jump of q across e, that is $[q] := (q|_{T'})|_e - (q|_{T''})|_e$, where T' and T'' are the triangles of $\mathcal{T}_h$ sharing the edge e. Moreover, let $\boldsymbol{v} \in \mathrm{L}^2(\Omega)^2$ such that $\boldsymbol{v}|_T \in C(T)^2$ for each $T \in \mathcal{T}_h$. Then, given $e \in \mathcal{E}_h(\Omega)$, we denote by $[\boldsymbol{v} \cdot \boldsymbol{t}]$ the tangential jump of $\boldsymbol{v}$ across e, that is, $[\boldsymbol{v} \cdot \boldsymbol{t}] := ((\boldsymbol{v}|_{T'})|_e - (\boldsymbol{v}|_{T''})|_e) \cdot \boldsymbol{t}_e$, where T' and T'' are the triangles of $\mathcal{T}_h$ sharing the edge e.

Next, let $k \geq 1$ be an integer and let $\mathbf{Z}_h, \mathbf{Q}_h$ and $\mathbf{U}_h$ be given by (4.1), (3.1), and (3.14), respectively. Let $(\omega, p) \in \mathbf{Z} \times \mathbf{Q}$ and $(\omega_h, p_h) \in \mathbf{Z}_h \times \mathbf{Q}_h$ be the unique solutions to the continuous and discrete problems (2.9) and (3.4) with data satisfying $\boldsymbol{f} \in \mathrm{L}^2(\Omega)^2$ and $\boldsymbol{f} \in \mathrm{H}^1(T)^2$ for each $T \in \mathcal{T}_h$. We introduce for each $T \in \mathcal{T}_h$ the local *a posteriori* error indicator for $\delta \in (0,1]$ as

$$
\begin{aligned}
\widetilde{\boldsymbol{\eta}}_T^2 :=\ & h_T^{2(1+\delta)} \| \operatorname{rot}(\sqrt{\nu}\, \mathbf{curl}\, \omega_h + \nu^{-1/2} \omega_h \times \boldsymbol{\beta} - \boldsymbol{f}) - \nu^{-1/2}\, \sigma \omega_h \|_{0,T}^2 \\
& + h_T^{2(1+\delta)} \| \operatorname{div}(\boldsymbol{f} - \nu^{-1/2} \omega_h \times \boldsymbol{\beta} - \nabla p_h) \|_{0,T}^2 + \sum_{e \in \mathcal{E}(T)} h_e^{(1+2\delta)} \| [(\sqrt{\nu}\, \mathbf{curl}\, \omega_h + \nu^{-1/2} \omega_h \times \boldsymbol{\beta} - \boldsymbol{f}) \cdot \boldsymbol{t}] \|_{0,e}^2 \\
& + \sum_{e \in \mathcal{E}(T)} h_e^{(1+2\delta)} \| [(\boldsymbol{f} - \nu^{-1/2} \omega_h \times \boldsymbol{\beta} - \nabla p_h) \cdot \boldsymbol{n}] \|_{0,e}^2 \\
=:\ & h_T^{2(1+\delta)} \left(\|\mathcal{R}_1\|_{0,T}^2 + \|\mathcal{R}_2\|_{0,T}^2 \right) + \sum_{e \in \mathcal{E}(T)} h_e^{(1+2\delta)} \left(\| [\mathcal{J}_{h,1} \cdot \boldsymbol{t}] \|_{0,e}^2 + \| [\mathcal{J}_{h,2} \cdot \boldsymbol{n}] \|_{0,e}^2 \right),
\end{aligned}
$$

and define its global counterpart as

$$\tilde{\boldsymbol{\eta}} := \left\{ \sum_{T \in \mathcal{T}_h} \tilde{\boldsymbol{\eta}}_T^2 \right\}^{1/2}. \tag{4.2}$$

Let us now establish reliability and quasi-efficiency of (4.2).

4.1 Reliability

This subsection focuses on proving the reliability of the estimator in the L^2-norm, and we note that this bound holds for $\delta \in (0, 1]$.

Theorem 4.1 *There exists a positive constant C_{rel}, independent of the discretisation parameter h, such that*

$$\|\sigma^{1/2}(\omega - \omega_h)\|_{0,\Omega} + \|p - p_h\|_{0,\Omega} \leq C_{\mathrm{rel}}\,\tilde{\boldsymbol{\eta}}. \tag{4.3}$$

Proof. Note that

$$\mathcal{A}((e_\omega, e_p), (\theta, q)) = \mathcal{R}(\theta, q), \tag{4.4}$$

where the residual operator $\mathcal{R} : \mathbf{Z} \times Q \mapsto \mathbb{R}$ is given by

$$\begin{aligned}
\mathcal{R}(\theta, q) &= \mathcal{F}(\theta, q) - \mathcal{A}((\omega_h, p_h), (\theta, q)) \\
&= \left(\boldsymbol{f} - (\sqrt{\nu}\,\mathbf{curl}\,\omega_h + \nabla p_h) - \nu^{-1/2}(\omega_h \times \boldsymbol{\beta}), (\sqrt{\nu}\,\mathbf{curl}\,\theta + \nabla q) \right)_{0,\Omega} - \sigma(\omega_h, \theta)_{0,\Omega}.
\end{aligned}$$

Integration by parts on this residual yields

$$\begin{aligned}
\mathcal{R}(\theta, q) &= \sum_{T \in \mathcal{T}_h} (\mathrm{rot}(\sqrt{\nu}\,\mathbf{curl}\,\omega_h + \nu^{-1/2}\omega_h \times \boldsymbol{\beta} - \boldsymbol{f}) - \nu^{-1/2}\,\sigma\omega_h, \sqrt{\nu}\,\theta)_{0,T} \\
&\quad - \sum_{e \in \mathcal{E}_h} \langle (\sqrt{\nu}\,\mathbf{curl}\,\omega_h + \nu^{-1/2}\,\omega_h \times \boldsymbol{\beta} - \boldsymbol{f}) \cdot \boldsymbol{t}, \sqrt{\nu}\,\theta \rangle_{0,e} \\
&\quad - \sum_{T \in \mathcal{T}_h} (\mathrm{div}(\boldsymbol{f} - \nu^{-1/2}\,\omega_h \times \boldsymbol{\beta} - \nabla p_h), q)_{0,T} + \sum_{e \in \mathcal{E}_h} \langle (\boldsymbol{f} - \nu^{-1/2}\,\omega_h \times \boldsymbol{\beta} - \nabla p_h) \cdot \boldsymbol{n}, q \rangle_{0,e} \\
&= \sum_{T \in \mathcal{T}_h} \left((\mathcal{R}_1, \sqrt{\nu}\,\theta)_{0,T} + (\mathcal{R}_2, q)_{0,T} \right) + \sum_{e \in \mathcal{E}_h} \left(\langle \mathcal{J}_{h,1} \cdot \boldsymbol{t}, \sqrt{\nu}\,\theta \rangle_{0,e} + \langle \mathcal{J}_{h,2} \cdot \boldsymbol{n}, q \rangle_{0,e} \right).
\end{aligned}$$

For the estimate (4.3), an appeal to the Aubin-Nitsche argument, using (3.9) with $(\theta, q) = (\omega - \omega_h, p - p_h)$ and $(\theta_h, q_h) = (\mathcal{N}_h \tilde{\omega}, \Pi_h \tilde{p}) \in \mathbb{V}_h$, now yields

$$\begin{aligned}
\sigma\,\|\omega - \omega_h\|_{0,\Omega}^2 + \|p - p_h\|_{0,\Omega}^2 &= \mathcal{A}((\omega - \omega_h, p - p_h), (\tilde{\omega}, \tilde{p})) \\
&= \mathcal{A}((\omega - \omega_h, p - p_h), (\tilde{\omega} - \theta_h, \tilde{p} - q_h)) \\
&= \mathcal{R}(\tilde{\omega} - \mathcal{N}_h \tilde{\omega}, \tilde{p} - \Pi_h \tilde{p}).
\end{aligned}$$

Then, we can rewrite the residual as

$$\begin{aligned}
\mathcal{R}(\tilde{\omega} - \mathcal{N}_h \tilde{\omega}, \tilde{p} - \Pi_h \tilde{p}) &= \sum_{T \in \mathcal{T}_h} \left((\mathcal{R}_1, \sqrt{\nu}\,(\tilde{\omega} - \mathcal{N}_h \tilde{\omega}))_{0,T} + \sum_{e \in \mathcal{E}(T)} \langle \mathcal{J}_{h,1} \cdot \boldsymbol{t}, \sqrt{\nu}\,(\tilde{\omega} - \mathcal{N}_h \tilde{\omega}) \rangle_{0,e} \right) \\
&\quad + \sum_{T \in \mathcal{T}_h} \left((\mathcal{R}_2, \tilde{p} - \Pi_h \tilde{p})_{0,T} + \sum_{e \in \mathcal{E}(T)} \langle \mathcal{J}_{h,2} \cdot \boldsymbol{n}, (\tilde{p} - \Pi_h \tilde{p}) \rangle_{0,e} \right),
\end{aligned}$$

and an application of the Cauchy-Schwarz inequality together with the approximation properties (3.2), (3.3) and (3.10) completes the rest of the proof. $\qquad\square$

4.2 Efficiency

This subsection deals with the efficiency of the *a posteriori* error estimator in the weighted $\mathbb{V}$-norm depending on $\delta \in (0,1)$ (a result that we call quasi-efficiency), and a bound in the L^2-norm, valid for $\delta = 1$.

Theorem 4.2 (Quasi-efficiency) *There is a positive constant C_{eff}, independent of h, such that for $\delta \in (0,1]$*

$$C_{\mathrm{eff}}\, \widetilde{\boldsymbol{\eta}} \leq C\, \|h_{\mathcal{T}}^{\delta}(e_{\omega}, e_p)\|_{\mathbb{V}} + \text{h.o.t.},$$

where h.o.t. *denotes higher-order terms and $\|h_{\mathcal{T}_h}^{\delta}(e_{\omega}, e_p)\|_{\mathbb{V}} := \left(\sum_{T \in \mathcal{T}_h} \|h_T^{\delta}(e_{\omega}, e_p)\|_{\mathbb{V}(T)}^2 \right)^{1/2}.$*

The second efficiency result is stated as follows.

Theorem 4.3 (Efficiency) *There is a positive constant C_{eff}, independent of h, such that for $\delta = 1$*

$$C_{\mathrm{eff}}\, \widetilde{\boldsymbol{\eta}} \leq C\, \|(\sigma^{1/2} e_{\omega}, e_p)\|_{0,\Omega} + \text{h.o.t.}.$$

A major role in the proof of efficiency is played by element and edge bubbles (locally supported non-negative functions), whose definition we recall in what follows. For $T \in \mathcal{T}_h(\Omega)$ and $e \in \mathcal{E}(T)$, let ψ_T and ψ_e, respectively, be the interior and edge bubble functions defined as in, e.g., [1]. Let $\psi_T \in \mathcal{P}_3(T)$ with $\mathrm{supp}(\psi_T) \subset T$, $\psi_T = 0$ on ∂T and $0 \leq \psi_T \leq 1$ in T. Moreover, let $\psi_e|_T \in \mathcal{P}_2(T)$ with $\mathrm{supp}(\psi_e) \subset \Omega_e := \{T' \in \mathcal{T}_h(\Omega) : e \in \mathcal{E}(T')\}$, $\psi_e = 0$ on $\partial T \setminus e$, and $0 \leq \psi_e \leq 1$ in Ω_e. Again, let us recall an extension operator $E : C^0(e) \mapsto C^0(T)$ that satisfies $E(q) \in \mathcal{P}_k(T)$ and $E(q)|_e = q$ for all $q \in \mathcal{P}_k(e)$ and for all $k \in \mathbb{N} \cup \{0\}$.

We now summarise the properties of ψ_T, ψ_e and E. For a proof, see [1] or [33].

Lemma 4.1 *The following properties hold:*

(i) For $T \in \mathcal{T}_h$ and for $v \in \mathcal{P}_k(T)$, there is a positive constant C_1 such that

$$C_1^{-1}\, \|v\|_{0,T}^2 \leq \int_T \psi_T v^2\, dx \leq C_1 \|v\|_{0,T}^2,$$
$$C_1^{-1}\, \|v\|_{0,T}^2 \leq \|\psi v\|_{0,T}^2 + h_T^2 |\psi v|_{1,T}^2 \leq C_1 \|v\|_{0,T}^2.$$

(ii) For $e \in \mathcal{E}_h$ and $v \in \mathcal{P}_k(e)$, there exists a positive constant say C_1 such that

$$C_1^{-1}\, \|v\|_{0,e}^2 \leq \int_e \psi_e v^2\, ds \leq C_1 \|v\|_{0,e}^2.$$

(iii) For $T \in \mathcal{T}_h$ with $e \in \mathcal{E}(T)$ and for all $v \in \mathcal{P}_k(e)$, there is a positive constant again say C_1 such that

$$\|\psi_e^{1/2}\, E(v)\|_{0,T}^2 \leq C_1 h_e\, \|v\|_{0,e}^2.$$

Proof of Theorem 4.2. With the help of the $\mathrm{L}^2(T)^2$-orthogonal projection $\mathcal{P}_T^{\ell}$ onto $\mathcal{P}_{\ell}(T)^2$, for $\ell \geq k$, with respect to the weighted L^2-inner product $(\psi_T \boldsymbol{f}, \boldsymbol{g})$, for $\boldsymbol{f}, \boldsymbol{g} \in \mathrm{L}^2(T)^2$, it now follows that

$$\|\mathcal{R}_1\|_{0,T}^2 = \|\nu^{-1/2}\sigma\omega_h + \mathrm{rot}(\sqrt{\nu}\,\mathbf{curl}\,\omega_h + \nu^{-1/2}\omega_h \times \boldsymbol{\beta} - \boldsymbol{f})\|_{0,T}^2$$

$$\leq 2\Big(\|\mathrm{rot}\,\boldsymbol{f} - \mathcal{P}_T^{\ell}(\mathrm{rot}\,\boldsymbol{f})\|_{0,T}^2 + \|\mathcal{P}_T^{\ell}(\nu^{-1/2}\sigma\omega_h + \mathrm{rot}(\sqrt{\nu}\,\mathbf{curl}\,\omega_h + \nu^{-1/2}\omega_h \times \boldsymbol{\beta} - \boldsymbol{f}))\|_{0,T}^2 \Big).$$

For the second term on the right-hand side, a use of Lemma 4.1 shows that

$$\|\mathcal{P}_T^{\ell}(\nu^{-1/2}\,\sigma\omega_h + \mathrm{rot}(\sqrt{\nu}\,\mathbf{curl}\,\omega_h + \nu^{-1/2}\omega_h \times \boldsymbol{\beta} - \boldsymbol{f}))\|_{0,T}^2 = \|\mathcal{P}_T^{\ell}\mathcal{R}_1\|_{0,T}^2$$

$$\leq \|\psi_T^{1/2}\mathcal{P}_T^\ell \mathcal{R}_1\|_{0,T}^2 = (\psi_T \mathcal{P}_T^\ell \, \mathcal{R}_1, \mathcal{R}_1)_{0,T}.$$

In a similar manner, we can derive the bounds

$$\|\mathcal{R}_2\|_{0,T}^2 \leq 2\Big(\|\operatorname{div} \boldsymbol{f} - \mathcal{P}_T^\ell(\operatorname{div} \boldsymbol{f})\|_{0,T}^2 + \|\mathcal{P}_T^\ell \mathcal{R}_2\|_{0,T}^2\Big),$$

and

$$\|\mathcal{P}_T^\ell \mathcal{R}_2\|_{0,T}^2 \leq \|\psi_T^{1/2}\mathcal{P}_T^\ell \, \mathcal{R}_2\|_{0,T}^2 = (\psi_T \mathcal{P}_T^\ell \, \mathcal{R}_2, \mathcal{R}_2)_{0,T}.$$

We proceed to choose $(\theta, q) = \psi_T(\mathcal{P}_T^\ell \, \mathcal{R}_1, \mathcal{P}_T^\ell \, \mathcal{R}_2)$ in (4.4) and obtain

$$\|\psi_T^{1/2}\mathcal{P}_T^\ell \, \mathcal{R}_1\|_{0,T}^2 + \|\psi_T^{1/2}\mathcal{P}_T^\ell \, \mathcal{R}_2\|_{0,T}^2 = ((\mathcal{R}_1, \mathcal{R}_2), \psi_T(\mathcal{P}_T^\ell \, \mathcal{R}_1, \mathcal{P}_T^\ell \, \mathcal{R}_2))_{0,T}$$
$$= \mathcal{A}_T((e_\omega, e_p), \psi_T(\mathcal{P}_T^\ell \, \mathcal{R}_1, \mathcal{P}_T^\ell \, \mathcal{R}_2)). \tag{4.5}$$

Next, we invoke estimate (i) of Lemma 4.1. This yields

$$\|\psi_T^{1/2}\mathcal{P}_T^\ell \, \mathcal{R}_1\|_{0,T}^2 + \|\psi_T^{1/2}\mathcal{P}_T^\ell \, \mathcal{R}_2\|_{0,T}^2 \leq C \, \|(e_\omega, e_p)\|_{\mathbb{V}(T)} \, \|\psi_T \mathcal{P}_T^\ell \, (\mathcal{R}_1, \mathcal{R}_2)\|_{\mathbb{V}(T)}$$
$$\leq C \, h_T^{-1}\|(e_\omega, e_p)\|_{\mathbb{V}(T)} \left(\|\mathcal{R}_1\|_{0,T}^2 + \|\mathcal{R}_2\|_{0,T}^2\right)^{1/2}.$$

Altogether, we now arrive at

$$h_T^{2(1+\delta)} \left(\|\mathcal{R}_1\|_{0,T}^2 + \|\mathcal{R}_2\|_{0,T}^2\right) \leq C \left(\|h_T^\delta(e_\omega, e_p)\|_{\mathbb{V}(T)}^2 + h_T^{2(1+\delta)}(\|\operatorname{rot} \boldsymbol{f} - \mathcal{P}_T^\ell(\operatorname{rot} \boldsymbol{f})\|_{0,T}^2 \right.$$
$$\left. + \|\operatorname{div} \boldsymbol{f} - \mathcal{P}_T^\ell(\operatorname{div} \boldsymbol{f})\|_{0,T}^2)\right). \tag{4.6}$$

Regarding the estimates associated with $\mathcal{J}_{h,1}$ and $\mathcal{J}_{h,2}$, we introduce, respectively, $\widetilde{\mathcal{P}}_T^\ell$ and $\widetilde{\mathcal{P}}_e^\ell$ as the weighted L^2-orthogonal projections (say, with respect to the weighted inner product $(\psi_e f, g)_e$), onto $\mathcal{P}_\ell(T)^2$ and $\mathcal{P}_\ell(e)$, for $\ell \geq k$. Then, we can bound $\mathcal{J}_{h,1}$ and $\mathcal{J}_{h,2}$ as

$$h_e^{(1+2\delta)}\Big(\|[\mathcal{J}_{h,1} \cdot \boldsymbol{t}]\|_{0,e}^2 + \|[\mathcal{J}_{h,2} \cdot \boldsymbol{n}]\|_{0,e}^2\Big) \leq h_e^{(1+2\delta)}\Big(\|[(\boldsymbol{f} - \widetilde{\mathcal{P}}_T^\ell \boldsymbol{f}) \cdot \boldsymbol{t}]\|_{0,e}^2 + \|[(\boldsymbol{f} - \widetilde{\mathcal{P}}_T^\ell \boldsymbol{f}) \cdot \boldsymbol{n}]\|_{0,e}^2\Big)$$
$$+ h_e^{(1+2\delta)}\Big(\|[\widetilde{\mathcal{P}}_e^\ell(\mathcal{J}_{h,1}) \cdot \boldsymbol{t}]\|_{0,e}^2 + \|[\widetilde{\mathcal{P}}_e^\ell(\mathcal{J}_{h,2}) \cdot \boldsymbol{n}]\|_{0,e}^2\Big). \tag{4.7}$$

In order to estimate the first term on the right-hand side of (4.7) we use the trace inequality, yielding

$$h_e^{(1+2\delta)}\Big(\|[(\boldsymbol{f} - \widetilde{\mathcal{P}}_e^\ell \boldsymbol{f}) \cdot \boldsymbol{t}]\|_{0,e}^2 + \|[(\boldsymbol{f} - \widetilde{\mathcal{P}}_e^\ell \boldsymbol{f}) \cdot \boldsymbol{n}]\|_{0,e}^2\Big)$$
$$\leq C \, h_e^{(1+2\delta)} \sum_{T \in \Omega_e} \left(h_e^{-1}\|\boldsymbol{f} - \widetilde{\mathcal{P}}_e^\ell \boldsymbol{f}\|_{0,T}^2 + h_e\|\nabla(\boldsymbol{f} - \widetilde{\mathcal{P}}_e^\ell \boldsymbol{f})\|_{0,T}^2\right)$$
$$\leq C \sum_{T \in \Omega_e} \left(h_T^{2\delta}\|\boldsymbol{f} - \widetilde{\mathcal{P}}_e^\ell \boldsymbol{f}\|_{0,T}^2 + h_T^{2(1+\delta)}\|\nabla(\boldsymbol{f} - \widetilde{\mathcal{P}}_e^\ell \boldsymbol{f})\|_{0,T}^2\right). \tag{4.8}$$

Again from (4.4) we note that with $(\boldsymbol{\theta}, q) = \psi_e E([\widetilde{\mathcal{P}}_e^\ell \mathcal{J}_{h,1} \cdot \boldsymbol{t}], [\widetilde{\mathcal{P}}_e^\ell \mathcal{J}_{h,2} \cdot \boldsymbol{n}])_e$ we obtain

$$\mathcal{A}_T((e_\omega, e_p), \psi_e E([\widetilde{\mathcal{P}}_e^\ell \mathcal{J}_{h,1} \cdot \boldsymbol{t}], [\widetilde{\mathcal{P}}_e^\ell \mathcal{J}_{h,2} \cdot \boldsymbol{n}])_{0,e}) = ((\mathcal{R}_1, \mathcal{R}_2), \psi_e E([\widetilde{\mathcal{P}}_e^\ell \mathcal{J}_{h,1} \cdot \boldsymbol{t}], [\widetilde{\mathcal{P}}_e^\ell \mathcal{J}_{h,2} \cdot \boldsymbol{n}]))_{0,\Omega_e}$$
$$+ (([\mathcal{J}_{h,1} \cdot \boldsymbol{t}], [\mathcal{J}_{h,2} \cdot \boldsymbol{n}]), \psi_e E([\widetilde{\mathcal{P}}_e^\ell \mathcal{J}_{h,1} \cdot \boldsymbol{t}], [\widetilde{\mathcal{P}}_e^\ell \mathcal{J}_{h,2} \cdot \boldsymbol{n}]))_{0,e}.$$

Now we appeal again to Lemma 4.1 to readily find that

$$(([\mathcal{J}_{h,1} \cdot \boldsymbol{t}], [\mathcal{J}_{h,2} \cdot \boldsymbol{n}]), \psi_e E([\widetilde{\mathcal{P}}_e^\ell \mathcal{J}_{h,1} \cdot \boldsymbol{t}], [\widetilde{\mathcal{P}}_e^\ell \mathcal{J}_{h,2} \cdot \boldsymbol{n}]))_{0,e} \geq C_1 \left(\|[\widetilde{\mathcal{P}}_e^\ell \mathcal{J}_{h,1} \cdot \boldsymbol{t}]\|_{0,e}^2 + \|[\widetilde{\mathcal{P}}_e^\ell \mathcal{J}_{h,2} \cdot \boldsymbol{n}]\|_{0,e}^2\right),$$

and, thus, we arrive at

$$\left(\|[\widetilde{\mathcal{P}}_e^\ell \mathcal{J}_{h,1} \cdot \boldsymbol{t}]\|_{0,e}^2 + \|[\widetilde{\mathcal{P}}_e^\ell \mathcal{J}_{h,2} \cdot \boldsymbol{n}]\|_{0,e}^2\right) \leq C_1^{-1}\left(|\mathcal{A}_T((e_\omega, e_p), \psi_e E([\widetilde{\mathcal{P}}_e^\ell \mathcal{J}_{h,1} \cdot \boldsymbol{t}], [\widetilde{\mathcal{P}}_e^\ell \mathcal{J}_{h,2} \cdot \boldsymbol{n}])_{0,e})|\right.$$
$$\left. + |((\mathcal{R}_1, \mathcal{R}_2), \psi_e E([\widetilde{\mathcal{P}}_e^\ell \mathcal{J}_{h,1} \cdot \boldsymbol{t}], [\widetilde{\mathcal{P}}_e^\ell \mathcal{J}_{h,2} \cdot \boldsymbol{n}]))_{0,\Omega_e}|\right).$$

Therefore, employing properties (i) and (ii) from Lemma 4.1, it follows that

$$\left(\|[\widetilde{\mathcal{P}}_e^\ell \mathcal{J}_{h,1} \cdot \boldsymbol{t}]\|_{0,e}^2 + \|[\widetilde{\mathcal{P}}_e^\ell \mathcal{J}_{h,2} \cdot \boldsymbol{n}]\|_{0,e}^2\right) \leq C\left(\|(e_\omega, e_p)\|_{\mathbb{V}(\Omega_e)} \|\psi_e^{1/2} E([\widetilde{\mathcal{P}}_e^\ell \mathcal{J}_{h,1} \cdot \boldsymbol{t}], [\widetilde{\mathcal{P}}_e^\ell \mathcal{J}_{h,2} \cdot \boldsymbol{n}])\|_{\mathbb{V}(\Omega_e)}\right.$$
$$\left. + \|(\mathcal{R}_1, \mathcal{R}_2)\|_{0,\Omega_e} \|\psi_e^{1/2} E([\widetilde{\mathcal{P}}_e^\ell \mathcal{J}_{h,1} \cdot \boldsymbol{t}], [\widetilde{\mathcal{P}}_e^\ell \mathcal{J}_{h,2} \cdot \boldsymbol{n}])\|_{0,\Omega_e}\right)$$
$$\leq C\left(h_T^{-1} h_e^{1/2}\|(e_\omega, e_p)\|_{\mathbb{V}(\Omega_e)} + h_e^{1/2}\|(\mathcal{R}_1, \mathcal{R}_2)\|_{0,\Omega_e}\right)\left(\|[\widetilde{\mathcal{P}}_e^\ell \mathcal{J}_{h,1} \cdot \boldsymbol{t}]\|_{0,e}^2 + \|[\widetilde{\mathcal{P}}_e^\ell \mathcal{J}_{h,2} \cdot \boldsymbol{n}]\|_{0,e}^2\right)^{1/2}.$$

Now with $h_e \leq h_T$, we simply apply (4.6) and obtain

$$h_e^{\frac{1}{2}+\delta}\left(\|[\widetilde{\mathcal{P}}_e^\ell \mathcal{J}_{h,1} \cdot \boldsymbol{t}]\|_{0,e}^2 + \|[\widetilde{\mathcal{P}}_e^\ell \mathcal{J}_{h,2} \cdot \boldsymbol{n}]\|_{0,e}^2\right)^{1/2} \leq C\left(h_e^\delta \|(e_\omega, e_p)\|_{\mathbb{V}(\Omega_e)} + h_e^{1+\delta}\|(\mathcal{R}_1, \mathcal{R}_2)\|_{0,\Omega_e}\right)$$
$$\leq C\left(h_T^{2\delta}\|(e_\omega, e_p)\|_{\mathbb{V}(\Omega_e)}^2 + h_T^{2(1+\delta)}(\|\operatorname{rot}\boldsymbol{f} - \mathcal{P}_T^\ell(\operatorname{rot}\boldsymbol{f})\|_{0,T}^2 + \|\operatorname{div}\boldsymbol{f} - \mathcal{P}_T^\ell(\operatorname{div}\boldsymbol{f})\|_{0,T}^2)\right)^{1/2}. \quad (4.9)$$

Finally, we substitute (4.8) and (4.9) in (4.7), and then combine the result with (4.6) to complete the rest of the proof. $\qquad\square$

Proof of Theorem 4.3. We follow the same steps taken in the proof of Theorem 4.2 until arriving to relation (4.5). Then, applying integration by parts and exploiting the properties of ψ_T we can show

$$\|\psi_T^{1/2}\mathcal{P}_T^\ell \mathcal{R}_1\|_{0,T}^2 + \|\psi_T^{1/2}\mathcal{P}_T^\ell \mathcal{R}_2\|_{0,T}^2 = (\sigma^{1/2}e_\omega, \sigma^{1/2}\psi_T(\mathcal{P}_T^\ell \mathcal{R}_1))_{0,T}$$
$$+ (\sigma^{1/2}e_\omega \times \boldsymbol{\beta}, \sigma^{-1/2}\nu^{-1/2}(\mathbf{curl}(\psi_T\mathcal{P}_T^\ell \mathcal{R}_1) + \nabla(\psi_T\mathcal{P}_T^\ell \mathcal{R}_2)))_{0,T}$$
$$- (\sigma^{1/2}e_\omega, \sigma^{-1/2}(\nu\,\mathbf{curl}(\mathbf{curl}(\psi_T\mathcal{P}_T^\ell \mathcal{R}_1)))_{0,T} - (e_p, \Delta(\psi_T\mathcal{P}_T^\ell \mathcal{R}_2))_{0,T}. \quad (4.10)$$

An application of estimate (i) of Lemma 4.1 together with inverse inequality implies that

$$\|\psi_T^{1/2}\mathcal{P}_T^\ell \mathcal{R}_1\|_{0,T}^2 + \|\psi_T^{1/2}\mathcal{P}_T^\ell \mathcal{R}_2\|_{0,T}^2 \leq C\,h_T^{-2}\left(\|\sigma^{1/2}e_\omega\|_{0,T} + \|e_p\|_{0,T}\right)\left(\|\psi_T\mathcal{P}_T^\ell \mathcal{R}_1\|_{0,T} + \|\psi_T\mathcal{P}_T^\ell \mathcal{R}_2\|_{0,T}\right)$$
$$\leq C\,h_T^{-2}\|(\sigma^{1/2}e_\omega, e_p)\|_{0,T}\left(\|\mathcal{R}_1\|_{0,T}^2 + \|\mathcal{R}_2\|_{0,T}^2\right)^{1/2}.$$

Altogether, we now obtain

$$h_T^4\left(\|\mathcal{R}_1\|_{0,T}^2 + \|\mathcal{R}_2\|_{0,T}^2\right) \leq C\left(\|(\sigma^{1/2}e_\omega, e_p)\|_{0,T}^2 + h_T^4(\|\operatorname{rot}\boldsymbol{f} - \mathcal{P}_T^\ell(\operatorname{rot}\boldsymbol{f})\|_{0,T}^2\right.$$
$$\left. + \|\operatorname{div}\boldsymbol{f} - \mathcal{P}_T^\ell(\operatorname{div}\boldsymbol{f})\|_{0,T}^2)\right). \quad (4.11)$$

For the estimates of $\mathcal{J}_{h,1}$ and $\mathcal{J}_{h,2}$, we again proceed as in the proof of Theorem 4.2 to arrive at (4.7). Then, an integration by parts applied to the first term on the right-hand side of (4.7) as in (4.10), with estimates (i) and (ii) from Lemma 4.1, in combination with inverse inequality, and obvious cancellation, permit us to write

$$\left(\|[\widetilde{\mathcal{P}}_e^\ell \mathcal{J}_{h,1} \cdot \boldsymbol{t}]\|_{0,e}^2 + \|[\widetilde{\mathcal{P}}_e^\ell \mathcal{J}_{h,2} \cdot \boldsymbol{n}]\|_{0,e}^2\right)^{1/2} \leq C\left(h_T^{-2}\|(\sigma^{1/2}e_\omega, e_p)\|_{0,\Omega_e} + h_T^{1/2}\|(\mathcal{R}_1, \mathcal{R}_2)\|_{0,\Omega_e}\right).$$

Since $h_e \leq h_T$, we simply apply (4.11) to obtain, after squaring, the bound

$$h_e^3\left(\|[\widetilde{\mathcal{P}}_e^\ell \mathcal{J}_{h,1} \cdot \boldsymbol{t}]\|_{0,e}^2 + \|[\widetilde{\mathcal{P}}_e^\ell \mathcal{J}_{h,2} \cdot \boldsymbol{n}]\|_{0,e}^2\right) \leq C\left(\|(\sigma^{1/2}e_\omega, e_p)\|_{0,\Omega_e}^2 + h_T^4\|(\mathcal{R}_1, \mathcal{R}_2)\|_{0,\Omega_e}^2\right)$$

h	$\|\boldsymbol{\omega}-\boldsymbol{\omega}_h\|_{0,\Omega}$	rate	$\|p-p_h\|_{0,\Omega}$	rate	$\|\boldsymbol{u}-\boldsymbol{u}_h\|_{0,\Omega}$	rate	$\|\boldsymbol{u}-\tilde{\boldsymbol{u}}_h\|_{0,\Omega}$	rate	$\|(\boldsymbol{\omega},p)-(\boldsymbol{\omega}_h,p_h)\|_{\mathbb{V}}$	rate
				$k=1$						
1.414	5.1820	–	5.661091	–	2.812797	–	2.8105	–	12.9222	–
0.745	1.4824	1.954	0.601930	3.499	1.564395	0.916	2.3300	0.420	7.54263	0.840
0.380	0.5602	1.445	0.222225	1.480	0.871818	0.868	0.5504	2.143	4.99371	0.612
0.190	0.1222	2.196	0.047772	2.217	0.428659	1.024	0.1257	2.129	2.26335	1.141
0.096	0.0278	2.175	0.008442	2.548	0.212433	1.032	0.0321	2.005	1.10120	1.059
0.051	0.0074	2.082	0.002089	2.197	0.106335	1.088	0.0080	2.186	0.55034	1.091
0.028	0.0018	2.297	0.000489	2.377	0.053041	1.138	0.0019	2.282	0.27367	1.143
0.014	0.0004	2.184	0.000123	2.208	0.026735	1.097	0.0005	2.193	0.13906	1.084
				$k=2$						
1.414	1.603335	–	2.180130	–	3.4023	–	2.230100	–	9.7142	–
0.745	0.491516	1.846	0.195556	3.764	2.3595	1.028	0.316770	3.047	4.6790	1.140
0.380	0.057665	3.182	0.016245	3.695	0.4888	2.338	0.043145	2.961	0.8417	2.547
0.190	0.008520	2.758	0.001088	3.899	0.1180	2.050	0.005448	2.985	0.1939	2.117
0.096	0.001220	2.857	0.000042	4.768	0.0316	1.934	0.000629	3.175	0.0520	1.933
0.051	0.000155	3.241	0.000005	3.222	0.0078	2.200	0.000081	3.233	0.0127	2.218
0.028	0.000020	3.380	0.000001	3.465	0.0019	2.280	0.000010	3.401	0.0031	2.268
0.014	0.000002	3.375	1.34e-07	3.481	0.0004	2.203	0.000001	3.383	0.0008	2.203

Table 5.1: Example 1. Convergence tests against analytical solutions on a sequence of uniformly refined triangulations of the domain $\Omega = (-1,1)^2$. Approximations with $k=1,2$ and velocity postprocessing using (3.13) and (3.15).

$$\leq C\Big(\|(\sigma^{1/2}e_\omega, e_p)\|_{0,\Omega_e}^2 + h_T^4(\|\operatorname{rot}\boldsymbol{f} - \mathcal{P}_T^\ell(\operatorname{rot}\boldsymbol{f})\|_{0,T}^2 + \|\operatorname{div}\boldsymbol{f} - \mathcal{P}_T^\ell(\operatorname{div}\boldsymbol{f})\|_{0,T}^2)\Big). \tag{4.12}$$

On substitution of (4.12) and (4.8) in (4.7) for $\delta = 1$, it suffices to combine the resulting estimate with (4.11) to conclude the rest of the proof. $\square$

Remark 4.1 *Note that the a posteriori lower bound derived in Theorem 4.3 is valid only upon the assumption of H^2-regularity, that is, for $\delta = 1$. When $\delta \in (0,1)$, obtaining an efficiency result for the a posteriori error indicator in the L^2-norm is much more involved, essentially due to the presence of corner singularities. For instance, a reliable and efficient estimators using weighted L^2-norms is available for the Poisson equation in [34]. A similar analysis could eventually be carried out in the present case, provided an additional regularity is established using weighted Sobolev spaces and appropriate interpolation results. However here we restrict ourselves only to verifying these properties numerically in the next Section.*

In addition, the result of Theorem 4.2 does indicate that the estimator is quasi-efficient, as the error in the L^2-norm, $\|(\sigma^{1/2}e_\omega, e_p)\|_{0,\Omega}$, is proportional to $C\,\|(e_\omega, e_p)\|_{0,\Omega}$.

5 Numerical tests

In this section, we report the results of some numerical tests carried out with the finite element method proposed in Section 3. The solution of all linear systems is carried out with the multifrontal massively parallel sparse direct solver MUMPS.

The discrete formulation is extended to the case of mixed boundary conditions, assuming that the domain boundary is disjointly split into two parts Γ_1 and Γ_2 such that (2.5) is replaced by

$$\begin{aligned} \boldsymbol{u} &= \boldsymbol{g} && \text{on } \Gamma_1, \\ \boldsymbol{u} \times \boldsymbol{n} &= \boldsymbol{a} \times \boldsymbol{n} && \text{on } \Gamma_2, \end{aligned} \tag{5.1}$$

DoF	$\|\boldsymbol{u}-\boldsymbol{u}_h\|_{0,\Omega}$	rate	$\|\boldsymbol{u}-\tilde{\boldsymbol{u}}_h\|_{0,\Omega}$	rate	$\|(\sqrt{\sigma}e_{\boldsymbol{\omega}},e_p)\|_{0,\Omega}$	rate	$\|h^{\delta}_{\mathcal{T}_h}(e_{\boldsymbol{\omega}},e_p)\|_{\mathbb{V}}$	rate	$\text{eff}_1(\tilde{\boldsymbol{\eta}})$	$\text{eff}_2(\tilde{\boldsymbol{\eta}})$
$\delta=1/10$										
27	7.353-02	–	0.00371	–	0.08482	–	0.89616	–	0.0281	0.2964
83	3.02e-02	1.281	0.00096	1.947	0.02324	1.872	0.43461	1.044	0.0142	0.2668
291	1.14e-02	1.401	0.00023	2.056	0.00591	1.970	0.20478	1.086	0.00722	0.2498
1091	4.18e-03	1.453	5.66e-05	2.032	0.00149	1.993	0.09575	1.097	0.00374	0.2411
4227	1.50e-03	1.477	1.42e-05	2.015	0.00037	1.998	0.04467	1.099	0.00197	0.2367
16643	5.35e-04	1.493	3.48e-06	2.007	9.32e-05	2.001	0.02084	1.100	0.00105	0.2345
66051	1.90e-04	1.494	8.69e-07	2.003	2.33e-05	2.000	0.00972	1.100	0.000558	0.2334
263171	6.73e-05	1.500	2.17e-07	2.002	5.81e-06	2.000	0.00453	1.100	0.000298	0.2328
$\delta=1/2$										
27	7.35e-02	–	0.00371	–	0.08482	–	0.67910	–	0.0372	0.2398
83	3.02e-02	1.281	0.00096	1.958	0.02324	1.872	0.25282	1.449	0.0249	0.2382
291	1.14e-02	1.401	0.00023	2.056	0.00591	1.970	0.08912	1.492	0.0167	0.2395
1091	4.18e-03	1.453	5.66e-05	2.031	0.00149	1.993	0.03176	1.500	0.0114	0.2395
4227	1.50e-03	1.477	1.42e-05	2.025	0.00037	1.998	0.01152	1.500	0.0079	0.2395
16643	5.35e-04	1.493	3.48e-06	2.013	9.32e-05	2.001	0.00395	1.500	0.0055	0.2395
66051	1.90e-04	1.494	8.69e-07	2.000	2.33e-05	2.000	0.00147	1.500	0.0039	0.2395
263171	6.73e-05	1.500	2.17e-07	2.000	5.81e-06	2.000	0.00049	1.500	0.0027	0.2395
$\delta=1$										
27	7.35e-02	–	0.00371	–	0.0848	–	0.48022	–	0.0452	0.2390
83	3.02e-02	1.281	0.00096	1.958	0.0232	1.872	0.12480	1.942	0.0450	0.2397
291	1.14e-02	1.401	0.00023	2.056	0.00591	1.970	0.03152	1.991	0.0448	0.2395
1091	4.18e-03	1.453	5.66e-05	2.031	0.00149	1.993	0.00789	2.000	0.0448	0.2394
4227	1.50e-03	1.477	1.42e-05	2.025	0.00037	1.998	0.00197	2.000	0.0449	0.2395
16643	5.35e-04	1.493	3.48e-06	2.013	9.3e-05	2.001	0.00049	2.000	0.0448	0.2395
66051	1.90e-04	1.494	8.69e-07	2.000	2.33e-05	2.000	0.00012	2.000	0.0448	0.2395
263171	6.73e-05	1.500	2.17e-07	2.000	5.81e-06	2.000	3.08e-05	2.000	0.0448	0.2395

Table 5.2: Example 2A. Error history and effectivity indexes (5.2) associated with the *a posteriori* error estimator (4.2). Smooth solutions on the unit square. Approximation with $k = 1$, and velocity postprocessing using (3.13) and (3.15).

$$p = p_0 \qquad\qquad\qquad\qquad \text{on } \Gamma_2,$$

(see similar treatments in [13, 14]) and the condition of zero average is imposed on the Bernoulli pressure, using a real Lagrange multiplier approach, only if $\Gamma_2 = \emptyset$. Using (5.1), the linear functional $\mathcal{F}_h : \mathbb{V}_h \to \mathbb{R}$ defining the finite element scheme adopts the specification

$$\mathcal{F}(\boldsymbol{\theta}_h, q_h) = \int_{\Omega} \boldsymbol{f} \cdot (\sqrt{\nu}\,\mathbf{curl}\,\boldsymbol{\theta}_h + \nabla q_h) + \sigma\sqrt{\nu}\langle \boldsymbol{g} \times \boldsymbol{n}, \boldsymbol{\theta}_h\rangle_{\Gamma_1} - \sigma\langle \boldsymbol{g} \cdot \boldsymbol{n}, q_h\rangle_{\Gamma_1} + \sigma\sqrt{\nu}\langle \boldsymbol{a} \times \boldsymbol{n}, \boldsymbol{\theta}_h\rangle_{\Gamma_2}.$$

Example 1. First, we construct a manufactured solution in the two-dimensional domain $\Omega = (-1, 1)^2$ and assess the convergence properties and verify the rates anticipated in Lemma 3.2, and Theorems 3.2 and 3.3. We compute individual errors and convergence rates as usual for all fields on successively refined partitions of Ω. For this test we assume that Γ_1 is composed by the horizontal edges and the right edge, whereas Γ_2 is the rest of the boundary. We propose the following closed-form and smooth solutions

$$\boldsymbol{\omega}(x,y) := -\sqrt{\nu}\left(e^{x-1}\sin(\pi y)^2 + 2\pi^2(x - e^{x-1})(\sin(\pi y)^2 - \cos(\pi y)^2)\right), \quad p(x,y) := x^4 - y^4,$$

$$\boldsymbol{u}(x,y) := \begin{pmatrix} (e^{x-1} - x)(2\pi\sin(\pi y)\cos(\pi y)) \\ -(e^{x-1} - 1)(\sin(\pi y)^2) \end{pmatrix},$$

DoF	$\|e_{\boldsymbol{\omega}}\|_{0,\Omega}$	rate	$\|e_p\|_{0,\Omega}$	rate	$\|\boldsymbol{u}-\tilde{\boldsymbol{u}}_h\|_{0,\Omega}$	rate	$\|(\sqrt{\sigma}e_{\boldsymbol{\omega}},e_p)\|_{0,\Omega}$	rate	$\|h^{\delta}_{\mathcal{T}_h}(e_{\boldsymbol{\omega}},e_p)\|_{\mathbb{V}}$	rate	$\mathtt{eff}_1(\tilde{\boldsymbol{\eta}})$	$\mathtt{eff}_2(\tilde{\boldsymbol{\eta}})$
23	8.87e-05	–	1.19e-04	–	2.36e-04	–	0.00031	–	0.00100	–	0.0065	0.0215
53	0.000196	-1.90	6.92e-05	1.31	2.04e-04	0.35	0.00062	-1.72	0.00061	1.22	0.0344	0.0332
101	9.79e-05	2.16	3.36e-05	2.24	1.86e-04	0.28	0.00031	2.16	0.00024	2.74	0.0368	0.0295
151	6.11e-05	2.34	2.16e-05	2.18	1.10e-04	2.61	0.00019	2.34	0.00015	2.33	0.0672	0.0539
333	1.56e-05	3.46	8.83e-06	2.27	3.59e-05	2.84	5.01e-05	3.43	7.07e-05	2.02	0.0463	0.0654
625	6.55e-06	2.75	6.25e-06	1.10	1.64e-05	2.48	2.17e-05	2.66	5.08e-05	1.05	0.0414	0.0973
1493	3.08e-06	1.73	2.38e-06	2.21	7.87e-06	1.69	1.02e-05	1.76	2.39e-05	1.74	0.0408	0.0971
2837	1.55e-06	2.15	1.19e-06	2.14	4.01e-06	2.11	5.04e-06	2.15	1.32e-05	1.84	0.0362	0.0989
6285	6.99e-07	2.00	5.22e-07	2.09	1.83e-06	1.96	2.27e-06	2.01	6.74e-06	1.69	0.0345	0.1020
14631	3.42e-07	1.69	2.29e-07	2.03	8.24e-07	1.90	1.11e-06	1.71	3.24e-06	1.73	0.0340	0.1020
28095	1.81e-07	1.95	1.12e-07	2.09	4.50e-07	1.85	5.83e-07	1.95	1.86e-06	1.72	0.0318	0.1020
63113	8.46e-08	1.88	4.96e-08	2.02	2.02e-07	1.98	2.72e-07	1.88	9.23e-07	1.73	0.0295	0.1019

Table 5.3: Example 2B. Error history and effectivity indexes (5.2) associated with the *a posteriori* error estimator (4.2) using $\delta = 2/3$. Steep solutions on an L-shaped domain. Approximation with $k = 1$, and velocity postprocessing using (3.15).

satisfying $\boldsymbol{u} = \boldsymbol{0}$ on Γ_1. In addition, we consider

$$\boldsymbol{\beta}(x,y) := \left(\begin{array}{c} \frac{1}{6}(e^{x-1}-x)(\pi\sin(2\pi y)) \\ -(e^{x-1}-1)(\sin(\pi y)^2) \end{array} \right),$$

together with the model parameters $\sigma = 100$ and $\nu = 0.1$, which in turn fulfil (2.16). These exact solutions lead to a nonzero right-hand side that we use to verify the accuracy of the finite element approximation.

We report in Table 5.1 the error history of the method in the L^2- and $\mathbb{V}$-norms, where we also show the convergence of the post-processed velocity using the direct computation (3.13) producing $\boldsymbol{u}_h \in \mathbf{U}_h$, and the alternative post-processing through solving the auxiliary problem (3.15), giving $\tilde{\boldsymbol{u}}_h \in \widetilde{\mathbf{U}}_h$. It can be clearly seen that optimal order of convergence is reached for all fields in both polynomial degrees $k = 1$ and $k = 2$, which confirms the sharpness of the theoretical error bounds.

Example 2. Secondly, we test the properties of the *a posteriori* error estimator (4.2), including the reliability, efficiency, as well as quasi-efficiency of the estimator. In a first instance (Example 2A) we simply compute locally the estimator and check, using smooth exact solutions in a convex domain $\Omega = (0,1)^2$, how it relates to the true error, by refining uniformly the mesh. Defining the smooth function $\varphi(x,y) := x^2(1-x)^2y^2(1-y)^2$, the closed-form solutions are

$$\boldsymbol{u}(x,y) := \mathbf{curl}\,\varphi, \quad p(x,y) := x^4 - y^4, \quad \boldsymbol{\omega}(x,y) := \sqrt{\nu}\,\mathbf{curl}\,\boldsymbol{u},$$

and we take $\nu = 10^{-3}$, $\sigma = 10$, and $\boldsymbol{\beta}(x,y) := \mathbf{curl}\,\varphi$. Only Dirichlet velocity conditions are considered in this example (that is, Γ_2 is empty), which amounts to add a real Lagrange multiplier imposing the condition of zero-average for the Bernoulli pressure. In Table 5.2 we collect the error history of the method, including individual errors and convergence rates as well as the errors analysed in Theorems 4.1, 4.2, 4.3. As the estimator and the quasi-efficiency depend on the values of δ, we explore three cases $\delta \in \{1/10, 1/2, 1\}$. The robustness is assessed by computing the effectivity indexes as the ratios

$$\mathtt{eff}_1 := \frac{\|(\sigma^{1/2}e_{\boldsymbol{\omega}},e_p)\|_{0,\Omega}}{\tilde{\boldsymbol{\eta}}}, \qquad \mathtt{eff}_2 := \frac{\|h^{\delta}_{\mathcal{T}_h}(e_{\boldsymbol{\omega}},e_p)\|_{\mathbb{V}}}{\tilde{\boldsymbol{\eta}}}. \tag{5.2}$$

The results confirm that the estimator is robust with respect to the weighted $\mathbb{V}$-norm for all values of δ, but the second-last column of the table indicates that $\tilde{\boldsymbol{\eta}}$ is not necessarily efficient in the L^2-norm, for $\delta < 1$.

Next, as Examples 2B and 2C, we consider exact solutions with higher gradients and see how the estimator performs guiding adaptive mesh refinement as well as restoring optimal convergence rates. For this we follow a standard procedure of solving the discrete problem $\to$ estimating the error $\to$ marking cells for refinement
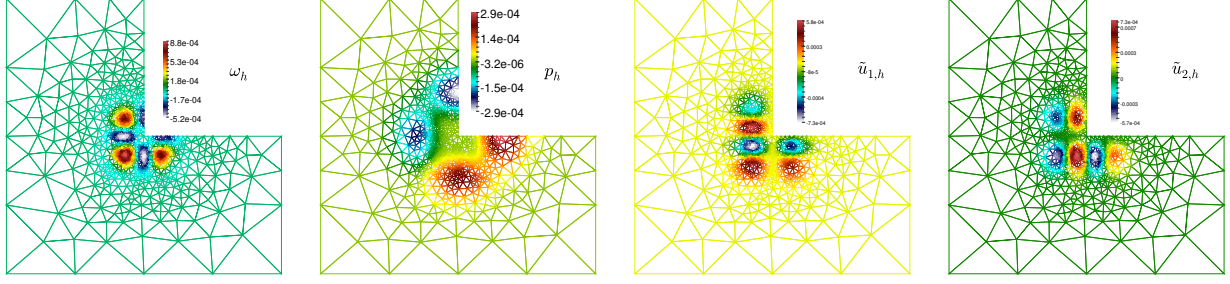
Figure 5.1: Example 2B. Approximate vorticity, Bernoulli pressure, and velocity components obtained from (3.15). Solutions computed after six steps of adaptive mesh refinement following (4.2) with $\delta = 2/3$.

$\rightarrow$ refining the mesh $\rightarrow$ solving again. The marking is based on the equi-distribution of the error in such a way that the diameter of each new element (contained in a generic triangle T on the initial coarse mesh) is proportional to the initial diameter times the ratio $\bar{\bar{\tilde{\boldsymbol{\eta}}}}_h/\boldsymbol{\eta}_T$, where $\bar{\bar{\tilde{\boldsymbol{\eta}}}}_h$ is the mean value of $\tilde{\boldsymbol{\eta}}$ over the initial mesh [33]. The refinement is then done on the marked elements as well as on an additional small layer in order to maintain the regularity of the resulting grid. An extra smoothing step is also applied after the refinement step.

For Example 2B we concentrate on the L-shaped domain $\Omega = (-1, 1)^2 \setminus (0, 1)^2$, and use the exact solutions

$$\varphi(x,y) := x^2(1-x)^2 y^2(1-y)^2 \exp(-50(x-0.01)^2 - 50(y-0.01)^2), \quad \boldsymbol{u}(x,y) := \mathbf{curl}\,\varphi,$$
$$p(x,y) := (x^5 - y^5)\exp(-25(x-0.01)^2 - 25(y-0.01)^2), \quad \boldsymbol{\omega}(x,y) := \sqrt{\nu}\,\mathbf{curl}\,\boldsymbol{u},$$

employed also to compute boundary data and right-hand side forcing terms. We keep the values of ν, σ from Example 1. The regularity of the coupled problem (due to the corner singularity) indicates that $\delta = 2/3$. We collect the results in Table 5.3, showing similar trends as those seen in Table 5.2, that is, optimal convergence for all fields, and robustness of the *a posteriori* error estimator in the $\mathbb{V}$-norm. Samples of approximate vorticity, Bernoulli pressure, and post-processed velocity, also for the case of $\delta = 2/3$, and after six steps of adaptive mesh refinement are shown in Figure 5.1.

For Example 2C, starting from a coarse initial triangulation of the domain, we construct sequences of uniformly and adaptively refined meshes and compute errors between approximate solutions and the following closed-form solutions exhibiting a vertical inner layer near the central axis of the domain (see [11])

$$\varphi(x,y) := x^2(1-x)^2 y^2(1-y)^2[1 - \tanh(150(1/2 - x))], \quad \boldsymbol{u}(x,y) := \mathbf{curl}\,\varphi,$$
$$p(x,y) := e^{-(x-1/2)^2} - p_0, \quad \boldsymbol{\omega}(x,y) := \sqrt{\nu}\,\mathbf{curl}\,\boldsymbol{u},$$

where p_0 is such the average of p over Ω is zero, and we take $\nu = 10^{-4}$, $\sigma = 10$, and $\boldsymbol{\beta}(x,y) := \mathbf{curl}\,\varphi$. Again we take Dirichlet velocity conditions everywhere on $\partial\Omega$.

Figure 5.2 shows the error history in both cases, confirming that the method constructed upon adaptive mesh refinement provides rates of convergence slightly better than the theoretical optimal, whereas under uniform refinement the lack of smoothness in the exact solutions hinder substantially the error decay, exhibiting sublinear convergence in all cases and even stagnating for vorticity. The top left plot portrays the individual errors, and for reference the optimal error decay for the case of less regular solutions (that is, $O(h)$); whereas the right panel shows the error in the $\mathbb{V}$-norm and the effectivity index $\mathtt{eff}_2$ defined in (5.2). In addition, the bottom panels of Figure 5.2 display the outputs of mesh refinement indicating a higher concentration of elements where the large gradients are located.

Example 3. Next, we conduct the well-known test of flow past a backward-facing step. This is also a 2D example where the domain is $\Omega = (0,6) \times (0,2) \setminus (0,1)^2$. For this case we choose a method with $k = 2$

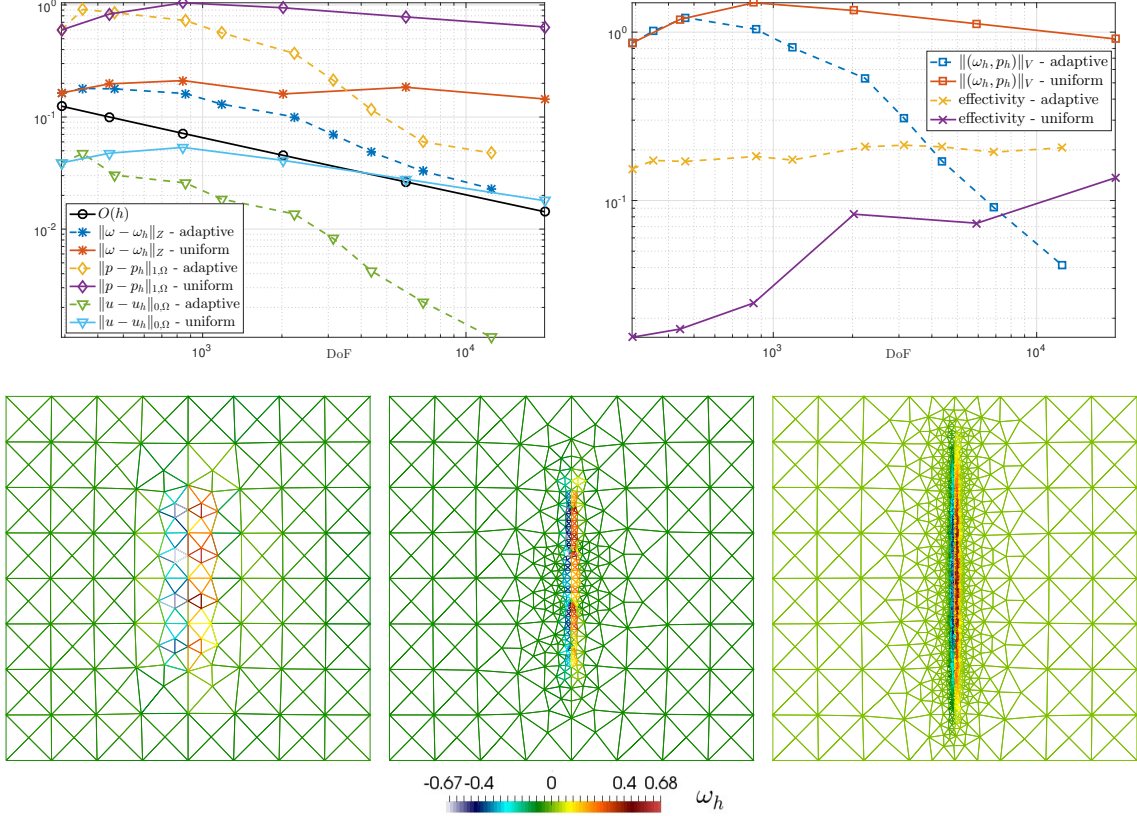Figure 5.2: Example 2C. Error decay in different norms and effectivity index `eff`$_2$ for the finite element approximation of the Oseen equations having an inner layer. Comparison plots between uniform (solid lines) and adaptive (dashed lines) mesh refinement using the lowest-order scheme (top panels); and examples of meshes produced after one, three, and six steps of adaptive refinement (bottom row).

and assume that $\boldsymbol{\beta}$ is the discrete velocity at the previous time iteration of a backward Euler time step. Assuming that no external forces are applied, we then have $\boldsymbol{f} = \sigma\boldsymbol{\beta}$ and after each time step characterised by $\sigma = (\Delta t)^{-1} = 100$, we update the current velocity $\boldsymbol{\beta} \leftarrow \boldsymbol{u}$. The flow regime is determined by a moderate viscosity $\nu = 0.05$ and we prescribe Γ_2 as the right edge (the outlet of the channel) where we set $p_0 = 0$ and $\boldsymbol{a} = \boldsymbol{0}$. The remainder of the boundary constitutes Γ_1: on the left edge (the inlet of the channel) we impose a parabolic profile $\boldsymbol{g} = (4(y-1)(2-y), 0)^T$ and on the remainder of Γ_1 (the channel walls) we set $\boldsymbol{g} = \boldsymbol{0}$. The system is run until the final time $t = 1$ and samples of the obtained numerical results are collected in Figure 5.3. As expected for this test, a fully developed profile (seen in the plot of post-processed velocity) exits the outlet while an important recirculation occurs on the bottom-left corner, right after the expanding region. The vorticity has a very high gradient on the reentrant corner of the channel, but this is well-captured by the numerical scheme. We also show Bernoulli pressure and the classical pressure (which coincides with the expected pressure profiles for this example). In addition, in Figure 5.4 we portray examples of adaptively refined meshes using the indicator (4.2). One can observe local refinement near the reentrant corner and at later times, a clustering of elements near the horizontal walls in the channel.

Example 4. For our next application we study the flow patterns generated on a channel with three obstacles (using the domain and boundary configuration from the micro-macro models introduced in [31]). Here the flow is now generated only through pressure difference between the inlet (the bottom horizontal section of the boundary defined by $(0, 1) \times \{-2\}$) and the outlet (the vertical segment on the top left part of the boundary,
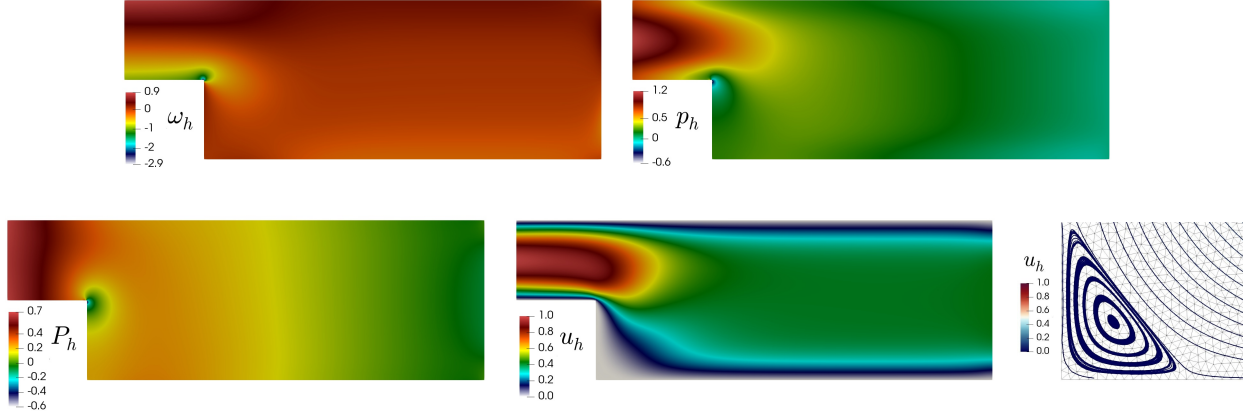
Figure 5.3: Example 3. Flow over a backward-facing step. Vorticity, Bernoulli pressure, true pressure, post-processed velocity, and zoom-in on bottom-left corner with velocity streamlines.
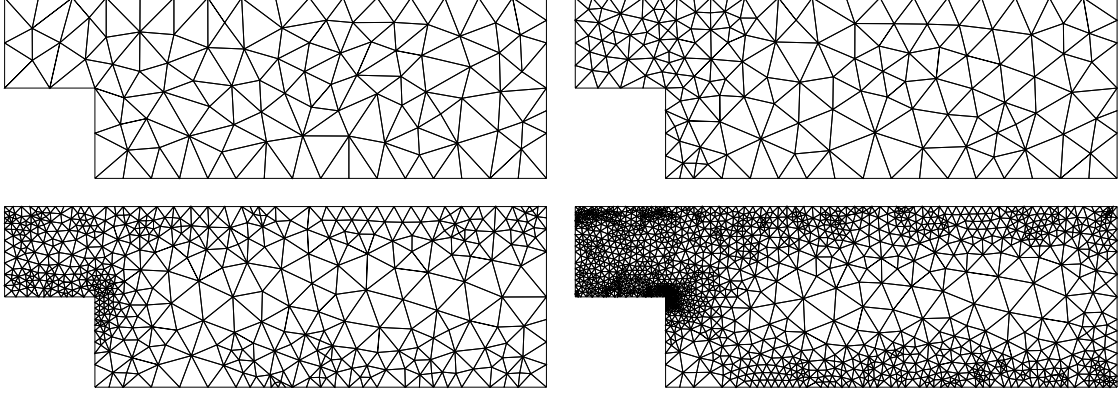

Figure 5.4: Example 3. Flow over a backward-facing step. Adaptively refined meshes according to the *a posteriori* error indicator (4.2), applying up to four refinement steps (from top-left to right-bottom).

defined by $\{-2\} \times (0,1)$). No other boundary conditions are set. As in the previous test case, $\boldsymbol{\beta}$ is the discrete velocity at the previous pseudo-time iteration. We take $\sigma = 10$ and $\nu = 0.02$ and increase the pressure at the inlet with the pseudo time, reaching after 10 steps the value $p_{in} = 3$ and set zero Bernoulli pressure at the outlet. The avoidance of the obstacles and accumulation of vorticity near them is a characteristic behaviour of the phenomenon that we can observe in Figure 5.5. These plots were generated with $k = 2$.

Example 5. Our last test exemplifies the performance of the numerical scheme in 3D. We use as computational domain the geometry of a femoral end-to-side bypass segmented from 3T MRI scans [26]. We generate a volumetric mesh of 68351 tetrahedra. The boundaries of this arterial bifurcation are considered as an inlet Γ_{in}, an outlet Γ_{out}, the arterial wall Γ_{wall}, and an occluded section Γ_{occl}. On the occlusion section and on the walls we set no-slip velocity. A parabolic velocity profile is considered at the inlet surface whereas a mean pressure distribution is prescribed on the outlet section. The last two conditions are time-dependent and periodic with a period of 50 time steps (we employ $\sigma = 100$ and run the system for 100 time steps). Moreover we use a blood viscosity of $\nu = 0.035$ (in g/cm^3), which represents an average Reynolds number between 144 and 380 [26]. The computations were carried out with the first-order scheme, and the results are
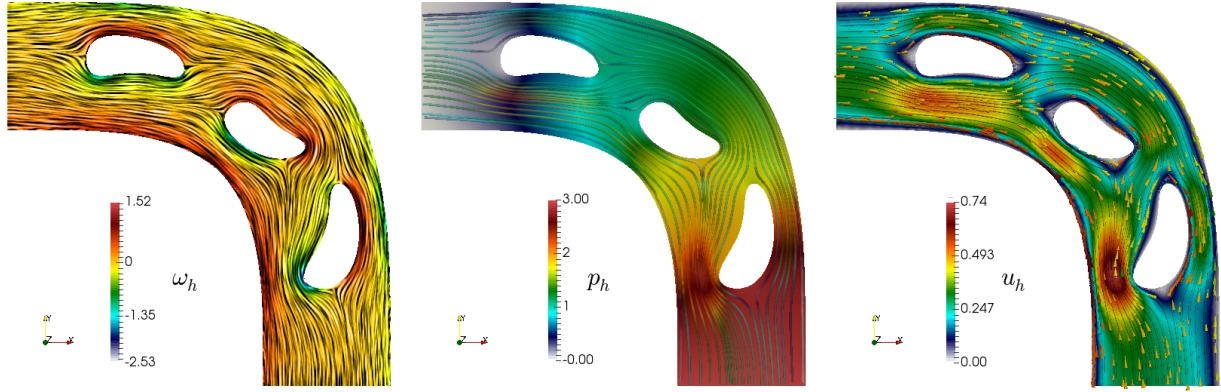
Figure 5.5: Example 4. Flow inside a channel with obstacles. Vorticity and line integral contours, classical pressure together with velocity streamlines, and post-processed velocity magnitude and arrows. Computation done with a second-order method.

shown in Figure 5.6, focusing on the solutions after 50 time steps. A relatively small zone with a secondary flow forms near the bifurcation, while the bulk stream continues towards the outlet.

References

[1] M. AINSWORTH AND J.T. ODEN, *A posteriori error estimation in finite element analysis.* Wiley, New York, 2000.

[2] A. ALONSO AND A. VALLI, *An optimal domain decomposition preconditioner for low-frequency time harmonic Maxwell equations.* Math. Comp., 68 (1999) 607–631.

[3] A. ALTAMIRANO-FERNANDEZ, J.G. VERGANO-SALAZAR, AND I. DUARTE-GANDICA, *Model of approximation of a velocity, vorticity and pressure in an incompressible fluid.* J. Phys.: Conference Series, 1514 (2020) e12002.

[4] M. ALVAREZ, G.N. GATICA, AND R. RUIZ-BAIER, *A posteriori error analysis of a fully-mixed formulation for the Brinkman-Darcy problem.* Calcolo, 54(4) (2017) 1491–1519.

[5] M. AMARA, D. CAPATINA-PAPAGHIUC, AND D. TRUJILLO, *Stabilized finite element method for Navier-Stokes equations with physical boundary conditions.* Math. Comp., 76(259) (2007) 1195–1217.

[6] K. AMOURA, M. AZAÏEZ, C. BERNARDI, N. CHORFI, AND S. SAADI, *Spectral element discretization of the vorticity, velocity and pressure formulation of the Navier-Stokes problem.* Calcolo, 44(3) (2007) 165–188.

[7] V. ANAYA, A. BOUHARGUANE, D. MORA, C. REALES, R. RUIZ-BAIER, N. SELOULA, AND H. TORRES, *Analysis and approximation of a vorticity-velocity-pressure formulation for the Oseen equations.* J. Sci. Comput., 80(3) (2019) 1577–1606.

[8] V. ANAYA, D. MORA, R. OYARZÚA, AND R. RUIZ-BAIER, *A priori and a posteriori error analysis for a mixed scheme for the Brinkman problem.* Numer. Math., 133 (2016) 781–817.

[9] V. ANAYA, D. MORA, AND R. RUIZ-BAIER, *Pure vorticity formulation and Galerkin discretization for the Brinkman equations.* IMA J. Numer. Anal., 37(4) (2017) 2020–2041.

[10] M. AZAÏEZ, C. BERNARDI, AND N. CHORFI, *Spectral discretization of the vorticity, velocity and pressure formulation of the Navier-Stokes equations.* Numer. Math., 104(1) (2006) 1–26.
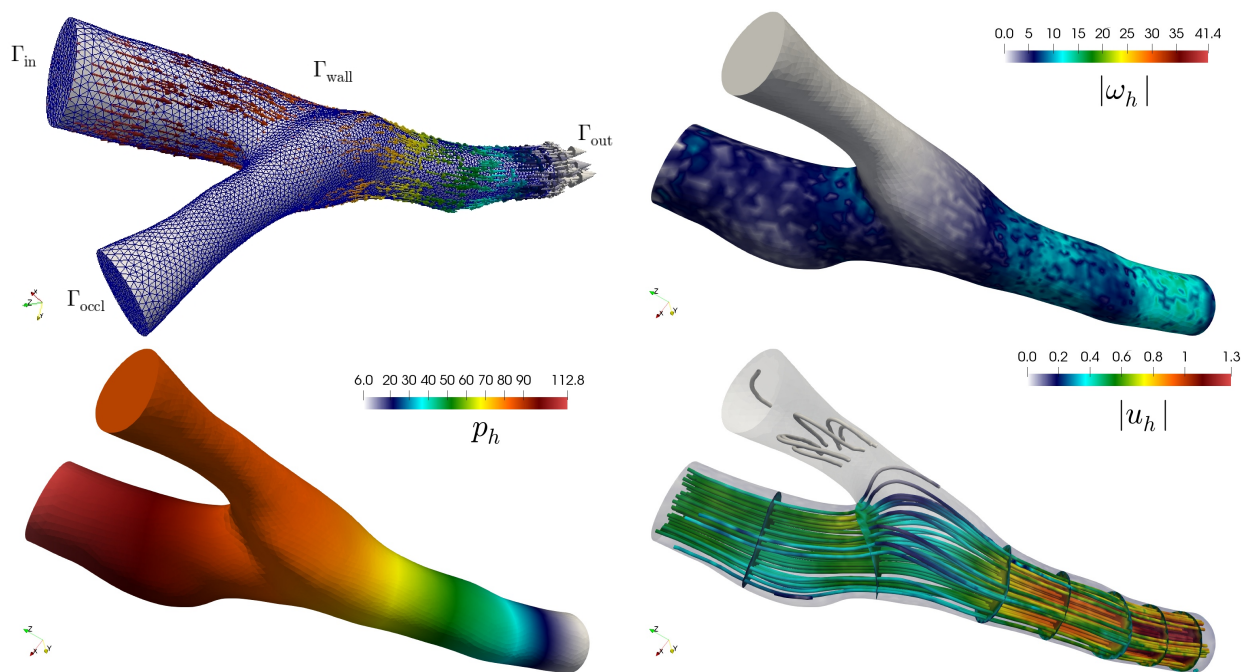
Figure 5.6: Example 5. Bifurcation flow on a femoral bypass geometry. These computations were performed using our first-order scheme.

[11] T. Barrios, J.M. Cascón, and M. González, *Augmented mixed finite element method for the Oseen problem: a priori and a posteriori error analyses*. Comput. Methods Appl. Mech. Engrg., 313 (2017) 216–238.

[12] M. Benzi, M.A. Olshanskii, L.G. Rebholz, and Z. Wang, *Assessment of a vorticity based solver for the Navier–Stokes equations*. Comput. Methods Appl. Mech. Engrg., 247-248 (2012) 216–225.

[13] C. Bernardi, T. Chacón, and D. Yakoubi, *Finite element discretization of the Stokes and Navier-Stokes equations with boundary conditions on the pressure*. SIAM J. Numer. Anal., 53(3) (2015) 1256–1279.

[14] S. Bertoluzza, V. Chabannes, C. Prud'homme, and M. Szopos, *Boundary conditions involving pressure for the Stokes problem and applications in computational hemodynamics*. Comput. Methods Appl. Mech. Engrg., 322 (2017) 58–80.

[15] P.B. Bochev, *Negative norm least-squares methods for the velocity-vorticity-pressure Navier-Stokes equations*. Numer. Methods PDEs, 15 (1999) 237–256.

[16] J. Camaño, G.N. Gatica, R. Oyarzúa, and G. Tierra, *An augmented mixed finite element method for the Navier-Stokes equations with variable viscosity*. SIAM J. Numer. Anal., 54 (2016) 1069–1092.

[17] C. Carstensen, A.K. Dond, N. Nataraj, and A.K. Pani, *Error analysis of nonconforming and mixed FEMs for second-order linear non-selfadjoint and indefinite elliptic problems*. Numer. Math., 133 (3) (2016) 557–597.

[18] C.L. Chang and S.-Y. Yang, *Analysis of the $[L^2, L^2, L^2]$ least-squares finite element method for incompressible Oseen-type problems*. Int. J. Numer. Anal. Model., 4(3-4) (2007) 402–424.

[19] A. Cesmelioglu, B. Cockburn, N.C. Nguyen, and J. Peraire, *Analysis of HDG methods for Oseen equations*. J. Sci. Comput., 55(2) (2013) 392–431.

[20] B. Cockburn, G. Kanschat, and D. Schötzau, *The local discontinuous Galerkin method for the Oseen equations*. Math. Comp., 73(246) (2004) 569–593.

[21] C. Davies and P.W. Carpenter, *A novel velocity-vorticity formulation of the Navier-Stokes equations with applications to boundary layer disturbance evolution*. J. Comput. Phys., 172 (2001) 119–165.

[22] H.-Y. Duan and G.-P. Liang, *On the velocity-pressure-vorticity least-squares mixed finite element method for the 3D Stokes equations*. SIAM J. Numer. Anal., 41(6) (2003) 2114–2130.

[23] F. Dubois, M. Salaün, and S. Salmon, *First vorticity-velocity-pressure numerical scheme for the Stokes problem.* Comput. Methods Appl. Mech. Engrg., 192(44–46) (2003) 4877–4907.

[24] G.N. Gatica, L.F. Gatica, and A. Márquez, *Augmented mixed finite element methods for a vorticity-based velocity–pressure–stress formulation of the Stokes problem in 2D.* Int. J. Numer. Methods Fluids, 67(4) (2011) 450–477.

[25] V. Girault and P.A. Raviart, *Finite element methods for Navier-Stokes equations. Theory and algorithms.* Springer-Verlag, Berlin, 1986.

[26] E. Marchandise, P. Crosetto, C. Geuzaine, J.-F. Remacle, and E. Sauvage, *Quality open source mesh generation for cardiovascular flow simulation.* In: D. Ambrosi, A. Quarteroni, and G. Rozza, editors. Modeling of Physiological Flows. Milano: Springer (2011) 395–414.

[27] S. Mohapatra and S. Ganesan, *A non-conforming least squares spectral element formulation for Oseen equations with applications to Navier-Stokes equations.* Numer. Funct. Anal. Optim., 37(10) (2016) 295–1311.

[28] M.A. Olshanskii, L.G. Rebholz, and A.J. Salgado, *On well-posedness of a velocity-vorticity formulation of the stationary Navier-Stokes equations with no-slip boundary conditions.* Discr. Cont. Dynam. Systems - A, 38(7) (2018) 3459–3477.

[29] M.A. Olshanskii and A. Reusken, *Navier-Stokes equations in rotation form: a robust multigrid solver for the velocity problem.* SIAM J. Sci. Comput., 23(5) (2002) 1683–1706.

[30] M. Salaün and S. Salmon, *Low-order finite element method for the well-posed bidimensional Stokes problem.* IMA J. Numer. Anal., 35(1) (2015) 427–453.

[31] M. Torrilhon and N. Sarna, *Hierarchical Boltzmann simulations and model error estimation.* J. Comput. Phys., 342(C) (2017) 66–84.

[32] C.-C. Tsai and S.-Y. Yang, *On the velocity-vorticity-pressure least-squares finite element method for the stationary incompressible Oseen problem.* J. Comput. Appl. Math., 182(1) (2005) 211–232.

[33] R. Verfürth, *A Review of A Posteriori Error Estimation and Adaptive-Mesh-Refinement Techniques.* Wiley-Teubner (Chichester), 1996.

[34] T.P. Wihler, *Weighted L^2-norm a posteriori error estimation of FEM in polygons*, Int. J. Numer. Anal. Model., 4 (2007) 100–115.